CHAPTER IV

RESULTS AND DISCUSSION

1. Formation of Daptomycin and PAMAM Dendrimer complexes

Typical mixtures of daptomycin and PAMAM dendrimer solutions were clear solutions. Although, some mixtures containing high PAMAM dendrimer concentration (0.20 to 0.70 mM) in a presence of phosphate buffer resulted in the precipitation. Typically titration mixtures were clear in all pH ranges. The characterization of the complex will be discussed further in details.

2. Selection of Characterization Techniques

2.1. Characterization of daptomycin and PAMAM dendrimer complex using ultrafiltration technique

Loss of daptomycin due to the ultrafiltration process was assessed by ultrafiltration of 0.02 to 0.10 mM daptomycin in 1.0 mM phosphate buffer. The solutions before and after ultrafiltration were immediately assayed using UV spectroscopy.

The UV spectrum of daptomycin showed three absorption maxima at 221, 260 and 280 nm (Figure 8). The absorption at 221 nm deviated from Beer's law in the concentration range used in this study; while at 260 and 280 nm the absorption were followed Beer's law. The 280 nm was chosen to be an analytical wavelength in this study and following study because it is an absorption wavelength of tryptophan residue on daptomycin. As depicted in Table 3 the observed percent recovery of daptomycin at various initial concentrations was 82 to 92 % and was independent of initial concentration.

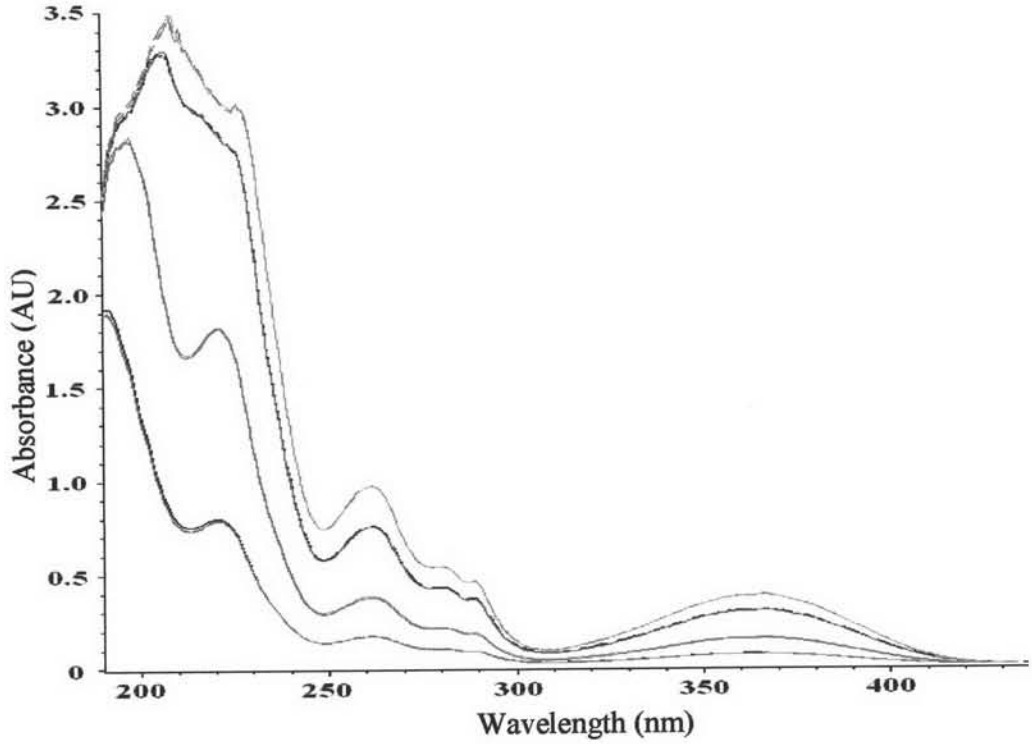

Figure 8 The UV spectra of daptomycin solutions at the concentration range of 0.02 to 0.10 mM

Table 3 Percent yield of daptomycin after ultrafiltration process at 2000 rpm for 15 minutes

Run #	Initial concentration of daptomcin (mM)	% yield
1	0.0200	92.23
2	0.0407	82.02
3	0.0806	83.90
4	0.1010	87.21

Loss of daptomycin in ultrafiltration process may be a result of either self aggregation of daptomycin or non-specific binding. Daptomycin was found to aggregate at high concentrations (Muangsiri, 2000). If the aggregates are larger than the molecular weight cut off (MWCO) of the ultrafiltration membrane, then they will be retained in the donor compartment. Consequently, the retained daptomycin can explain the low percent recovery. Alternatively, loss of daptomycin during ultrafiltration could be due to the non-specific binging of daptomycin to either the ultrafiltration membrane or the plastic surface

of ultrafiltration kits. In order to avoid the aggregation and non-specific binding of daptomycin during ultrafiltration process, daptomycin loss from blank solutions was used as correction factors for the complex characterization using ultrafiltration.

A preliminary study evaluating the use of ultrafiltration to measure complexation was conducted using daptomycin (0.02, 0.04, 0.08 and 0.10 mM) and PAMAM dendrimer generation 5 (0.47 mM) in phosphate buffer. The molecular weight of PAMAM dendrimer generation 5 and daptomycin is 28,853 and 1620 D, respectively, while the molecular weight cut-off for the ultrafiltration membrane was 10 kD. It was anticipated that only free daptomycin would pass through the membrane. The loss of free daptomycin in the ultrafiltrates was attributable to the complex formation and non-specific loss of daptomycin during ultrafiltration. The non-specific loss of daptomycin during ultrafiltration process was corrected by using control samples at each concentration of daptomycin.

The absorption spectra of all solutions were taken before and after ultrafiltration process using UV spectrometer. The UV spectra of ultrafiltrates from the mixtures showed baseline shift due to UV light scattering (Figure 43, Appendix B). Consequently, the adsorption data obtained at wavelength of 280 nm were variable and not used to determine the free concentration of daptomycin. The UV light scattering was suspected to be due to the presence of either daptomycin aggregation. The further studies were attempted to improve the preliminary attempts at using the ultrafiltration technique.

2.1.1. Approaches for improving ultrafiltration technique

2.1.1.1. Control of daptomycin aggregation

10% acetonitrile was added the solvent to decrease daptomycin aggregation. The concentration range of daptomycin was extended to the higher concentration range (0.02 to 0.7 mM), whereas the concentration of PAMAM dendrimer generation 5 (0.47 mM) remained the same. The precipitation was observed in the solution mixtures containing higher daptomycin concentrations.

Daptomycin concentrations in ultrafiltrates were determined using UV spectrometer. The extent of baseline shift due to light-scattering from daptomycin aggregates decreased (Figure 9). Hence, the solvent modification of adding 10% acetonitrile appeared to prevent the daptomycin aggregation issue.

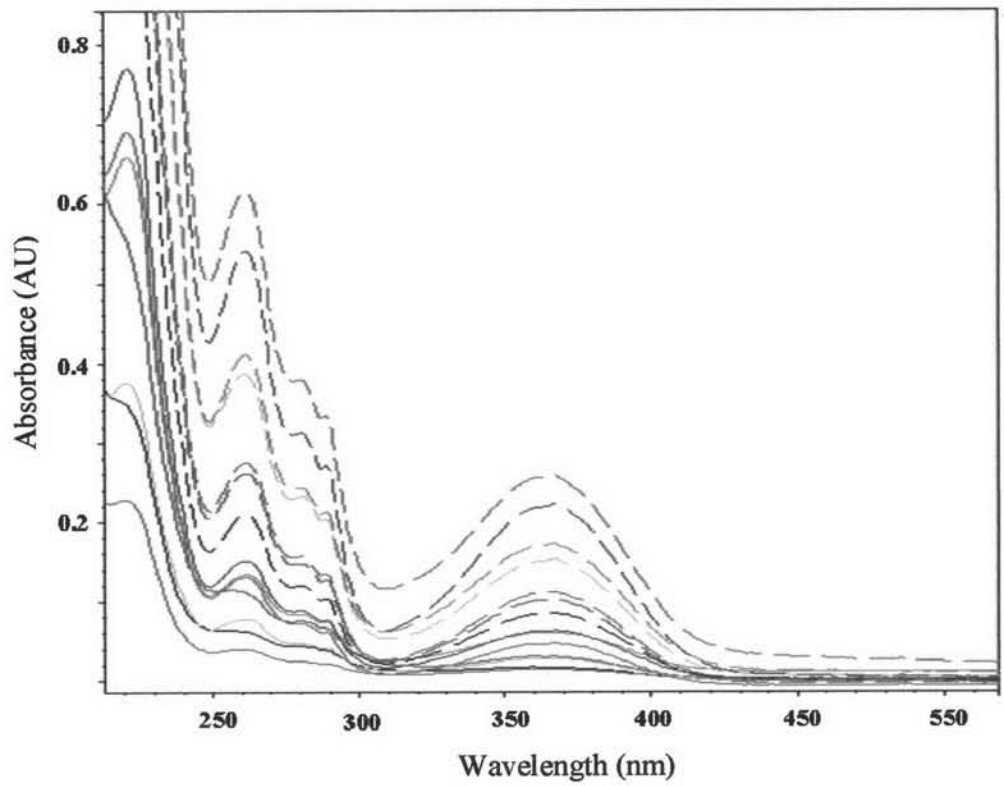

Figure 9 The UV spectra of ultrafiltrates obtained from the mixtures of 0.07 mM PAMAM dendrimer generation 5 and 0.02 to 0.7 mM daptomycin in 0.001 mM Phosphate buffer and 10% acetonitrile

The predicted loss of daptomycin upon ultrafiltration was expected to be the consequence of complex formation and non-specific binding of daptomycin. The loss of daptomycin due to non-specific binding during ultrafiltration was determined from control studies (Table 4). The total free daptomycin concentration was the summation of the free daptomycin concentration obtained from the ultrafiltrates and the loss of daptomycin during ultrafiltration obtained from control studies. The complex or bound concentration was calculated from the subtraction of initial daptomycin concentration by the total free daptomycin concentration.

Table 4 Bound concentration of daptomycin to PAMAM dendrimer generation 5 determined by ultrafiltration technique at 2000 rpm, 15 minutes

	Daptomycin concentration (mM)				
No.	Initial daptomycin	Loss of daptomycin by non-specific binding	Free daptomaycin from ultrafiltrates	Actual free daptomycin	Bound daptomycin
1	0.0198	0.0009	0.0093	0.0102	0.0096
2	0.0403	0.0038	0.0052	0.0090	0.0313
3	0.0501	0.0054	0.0152	0.0206	0.0295
4	0.0803	0.0097	0.0143	0.0240	0.0563
5	0.1001	0.1001	0.0089	0.0000	0.0089
6	0.2002	0.0429	0.1040	0.1469	0.0533
7	0.3004	0.0537	0.1972	0.2509	0.0495
8	0.4005	0.0763	0.2749	0.3512	0.0493
9	0.5006	0.1020	0.3840	0.4860	0.0146
10	0.7009	0.1772	0.5872	0.7644	-0.0635

The binding isotherm, the plot of relationship between complex daptomycin and total daptomycin concentration, was shown in Figure 8. At total daptomycin concentration lower than 0.1 mM, complex daptomycin concentration increased with increasing total daptomycin concentration. The complex concentration appeared to be independent of total daptomycin concentration in a range of 0.1 to 0.4 mM which implied that complex formation reached the saturation state. The complex concentration was inversely proportional to total daptomycin concentration. The observed negative deviation in complex concentration was suspected to be caused by two reasons; (i) the displacement of phosphate ion and (ii) the precipitation of the mixtures. Phosphate buffer was thought to be involved in aggregation of dendrimer leading to the observed precipitation. This assumption will be discussed later on in detail.

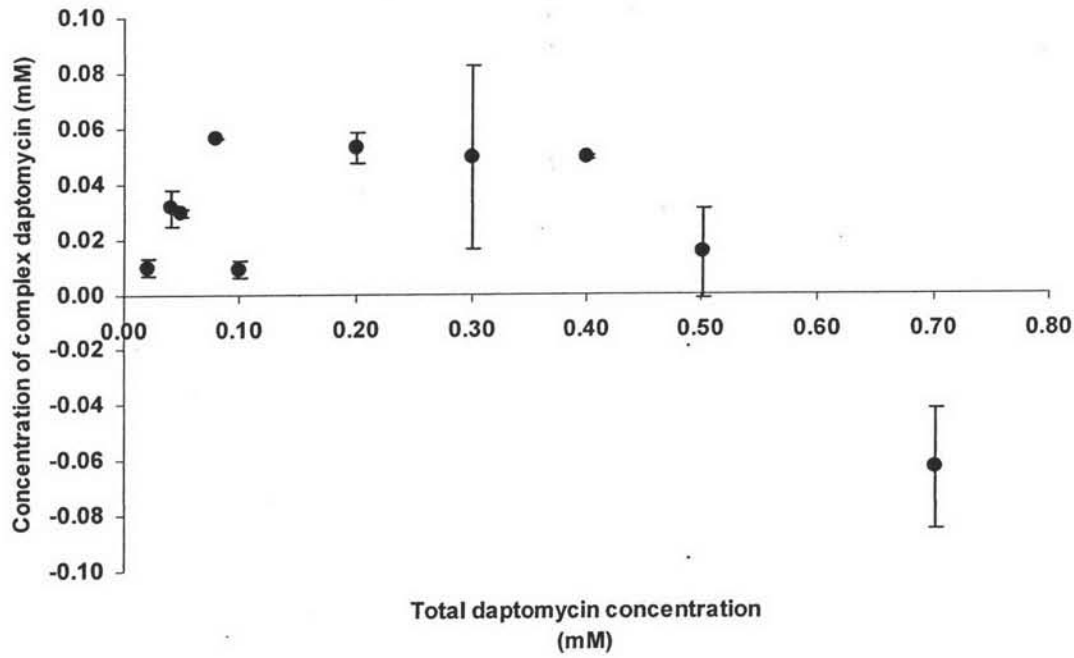

Figure 10 The binding isotherm of the interaction between daptomycin and PAMAM generation 5 characterized by ultrafiltration technique at various initial daptomycin concentration in a range of 0.02 to 0.7 mM

2.1.1.2 Determination of effect of phosphate on free concentration of daptomycin

In order to determine the effect of phosphate buffer on daptomycin binding, the formation of daptomycin-PAMAM complex in the absence of phosphate buffer were characterized using ultrafiltration technique at the same concentration range with previous study. The precipitation was not observed. Plot between complex daptomycin concentration and total daptomycin concentration (Figure 9) shows that the complex daptomycin concentrations appear to increase at low total daptomycin concentration and then gradually increase at high total daptomycin concentrations. However, the experimental data were very variable.

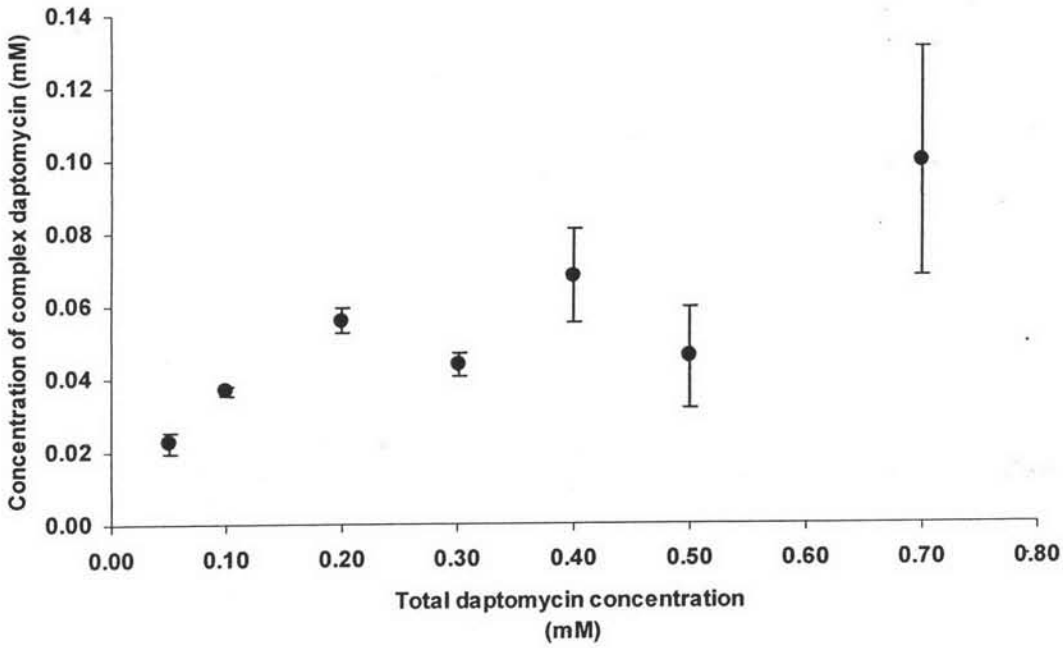

Figure 11 The binding isotherm of the interaction between daptomycin and PAMAM generation 5 characterized by ultrafiltration technique at various initial daptomycin concentration in a range of 0.05 to 0.7 mM without using phosphate buffer at pH 7.0

Dendrimer aggregation has been reported in studies on the interaction of PAMAM dendrimer and fluorescence probes, 1-(trimethylammoniumphenyl)-6-phenyl-1,3,5 hexatriene p-toluenesulfonate (TMA-DPH) and 1-anilino-8-naphthalene sulfonate (ANS) (Domaski, Klajnert and Bryszewska, 2004; Klajnert et al., 2006). Fluorescence probes were found to aggregate on the cationic surfaces of PAMAM dendrimer and enhance the self-association process of PAMAM dendrimer. Similarly, our results showed the bound concentration of daptomycin was less at the presence of phosphate buffer. It is possible that mono- and dibasic phosphate ions ($H_2PO_4^-$ and HPO_4^{2-}) associated with the cationic surface of PAMAM dendrimers and induced the PAMAM aggregation. This resulted the observed precipitation and an apparent reduction in the binding interaction between daptomycin and PAMAM dendrimer. Although this issue appeared to be obviated by avoiding the use of phosphate buffers, the binding data were variable and deemed to be unreliable our purposes.

2.1.1.3 Effect of the daptomycin and PAMAM dendrimer concentration on binding

In order to avoid the precipitation, the initial concentration of daptomycin and PAMAM dendrimer generation 5 reduced to 10 to 70 μM and 13.9 μM, respectively. The bound concentration of daptomycin increased, then reached the plateau and steeply increased again with increase in total daptomycin concentration as shown in figure 12 (close circle). This behavior is similar to adsorption isotherm type II (BET isotherm) which is explained by the multilayer adsorption. Consequently, the multilayer adsorption of daptomycin to the dendrimer molecule was suspected to appear in this system.

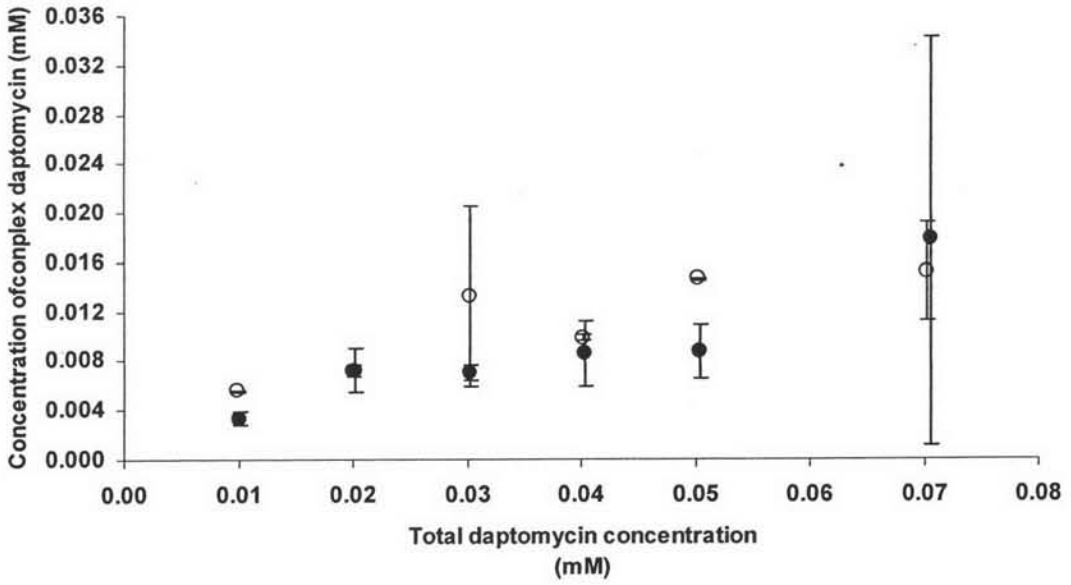

Figure 12 The binding isotherm of the interaction between daptomycin and PAMAM generation 5 characterized by ultrafiltration technique at various initial daptomycin concentration in a range of 0.1 to 0.7 mM without using phosphate buffer at pH 7.0 analyzed by UV spectrometer (close circle) and HPLC (opened circle)

At low concentration of daptomycin (10 to 70 μM), high performance liquid chromatography (HPLC) was needed in order to detect the low concentrations of recovered free daptomycin. The relationship between complex concentration and total daptomycin concentration is illustrated in Figure 10 (open circle).

The complex concentrations increased with increasing total daptomycin concentration and then attained a maximum value at total daptomycin concentration range of 0.01 to 0.07 mM.

2.1.1.4 Determination of optimized ultrafiltration operating parameters

Daptomycin (50 μM) solution was prepared in 10% acetonitrile and 0.001 mM Tris buffer. The solutions were ultrafiltrated in various operating conditions and the ultrafiltrate concentrations were analyzed using HPLC. The results reported in Table 5.

Table 5 Percent recovery of daptomycin after ultrafiltration process with various operating conditions designed by full factorial design with one center point

Run #	Force (x g)	Operating time (minutes)	Initial volume (mL)	% recovery
1	2000	25	0.8	64.59
2	2000	25	0.8	68.02
3	2000	25	0.4	56.16
4	2000	25	0.4	53.73
5	2000	15	0.8	57.88
6	2000	15	0.8	0.71
7	2000	15	0.4	44.22
8	2000	15	0.4	43.78
9	1500	25	0.8	61.75
10	1500	25	0.8	61.54
11	1500	25	0.4	70.67
12	1500	25	0.4	63.93
13	1500	15	0.8	56.08
14	1500	15	0.8	54.07
15	1500	15	0.4	70.17
16	1500	15	0.4	2.51
17	1750	20	0.6	56.16
18	1750	20	0.6	48.08

The prediction profile obtained from the linear model estimated using the data described in Table 5 (JMP software version 5.0.1, SAS institute) showed that the operating time appeared to have the largest effect on the percent recovery of daptomycin. On the contrary, the centrifugation force and initial volume did not effect to the percent recovery of daptomycin after ultrafiltration (Figure 13). Thus, the optimum operating parameters during ultrafiltration process is operating time of 25 minutes. In addition, none of interaction effects were statistically significant determinants of the percent daptomycin recovery. Under all conditions the percent recovery was $\leq$ 70% indicating that there was a significant loss of daptomycin. In this experiment because dendrimer was not present, failure to recover all of the daptomycin could be attributed to loss due to non-specific binding, retention of aggregated daptomycin or failure to recovery all of the filterable solution. Since non-specific binding is not likely to be affected by centrifugation force nor operating time and initial volume appears to have not effect on recovery variation, the major cause of incomplete daptomycin recovery was likely due to the failure of all of the filtrate to pass into the receptor compartment, i.e. some filterable solution remained in the donor compartment. Moreover, within each treatment condition, variable results were obtained, thus suggesting that this technique could not provide reliable quantitative binding information.

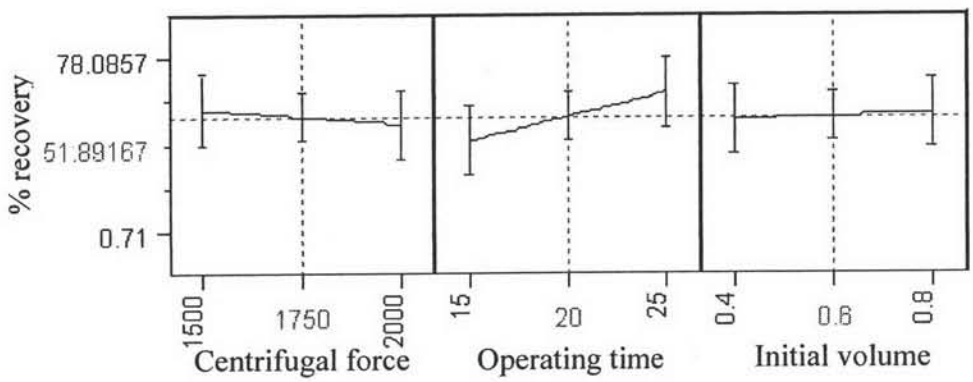

Figure 13 The full factorial analysis using JMP software version 5.0.1 (SAS institute) of the factorial model to degree 2.

2.1.2 Determination of dendrimer-daptomycin association constant

The binding results from ultrafiltration technique were not sufficiently reproducible to be used to determine an appropriate binding model and to estimate binding constants. However, other techniques such as UV difference technique and fluorescence spectroscopy technique were applied in order to determined complex formation.

2.2. Characterization of daptomycin and PAMAM dendrimer complex using UV difference spectroscopy

UV spectra of daptomycin in aqueous solution and in mixtures between various daptomycin concentrations and dendrimer are shown in Figure 14. UV spectrum of mixture at low concentrations of PAMAM dendrimer generation 5 (0.001 mM) was superimposed on that of free daptomycin spectrum. At high concentration of PAMAM dendrimer (0.01 to 0.05 mM), the baseline shift and slight roughness of spectra indicated UV scattering. The baseline correction was used to normalize the UV spectrum in order to get rid of the effect of UV scattering. The addition of PAMAM dendrimer generation 5 caused a slight increase in the absorbance in a range of 270 to 300 nm. However, the difference in the absorbance was insufficient to be used for accurate determination of dissociation constants.

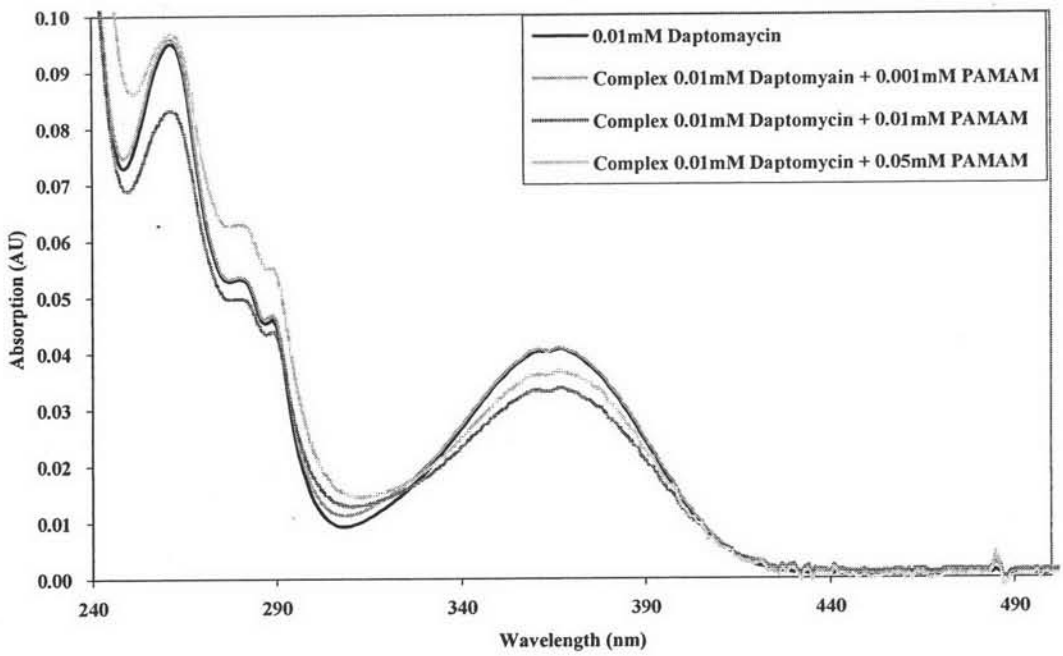

Figure 14 The UV spectra of daptomycin solution and daptomycin combined with 0.001, 0.01 and 0.05 mM PAMAM dendrimer generation 5

2.3. Characterization of daptomycin and PAMAM dendrimer complex using fluorescence spectroscopy

2.3.1. Determination of fluorescence response upon complex formation

Fluorescence emission spectra of 5 μM daptomycin in an absence of PAMAM excited at 260 and 285 nm showed maxima emission at 355 and 460 nm corresponding to emission wavelength of tryptophan and kynurenine, respectively (Figure 15). Solution containing PAMAM generation 5 showed no fluorescence emission maxima over the wavelength of 320 to 540 nm (Figure 44, Appendix B). The emission spectra resulting from excitation at 260 nm included a slight quenching of tryptophan fluorescence emission at 355 nm and a significant increase of kynurenine fluorescence emission at 460 nm were observed when PAMAM generation 5 was added to the aqueous solution of daptomycin (Figure 15a). In fact, the intensity of the kynurenine emission when excited at 260 with an emission slit width of 15 was over the detection limit. Excitation at 285 nm provided the optimum emission for probing the interaction between daptomycin and dendrimer in the concentration ranges of interest without exceeding the instrumentation limits (Figure 15b). In addition, an increase in emission slit width from 10 to 15 resulted in magnification of the relative fluorescence intensity and smoothness of the spectrum.

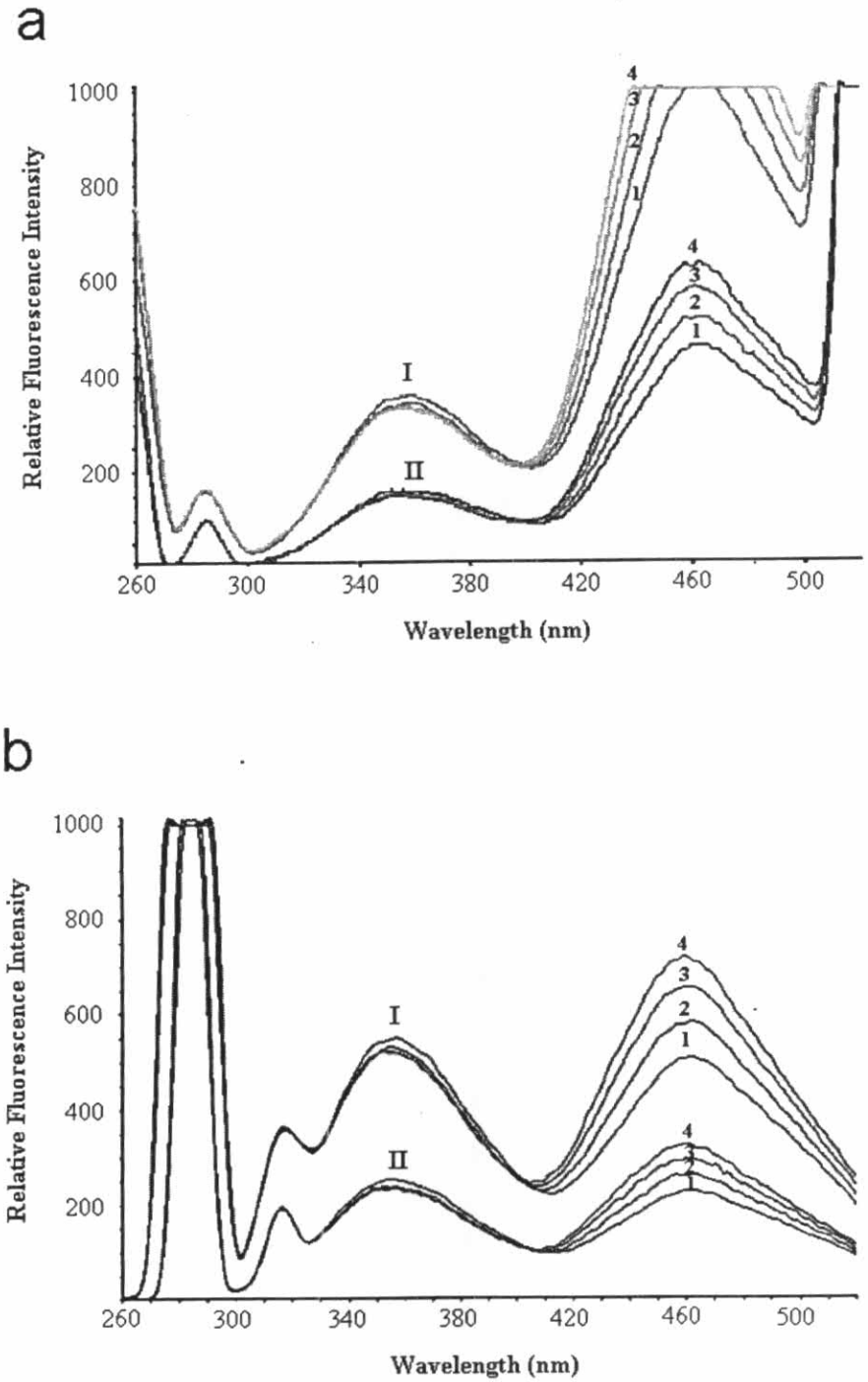

Figure 15 Fluorescence emission spectra of the mixtures between 5.0 μM daptomycin and (1) 0 μM, (2) 0.18 μM, (3) 0.36 μM, and (4) 0.54 μM PAMAM generation 5; (a) excitation at 260 nm and (b) excitation at 285 nm; (I) excitation/emission slit width 4/15 and (II) excitation/emission slit width 4/10

The observed kynurenine fluorescence enhancement upon PAMAM titration was due to either binding between daptomycin and PAMAM dendrimers or self-association of daptomycin. However additional studies using a variety of orthogonal analytical approaches including NMR, fluorescence and dynamic light-scattering have demonstrated that the minimum critical aggregation concentration (CAC) for daptomycin at any pH value is less than 100 μM (Qui and Kirsch, unpublished data). Therefore the fluorescence enhancements observed herein could be unequivocally attributed to daptomycin-dendrimer interactions because daptomycin concentrations in all studies were $\leq$ 5 μM. Similar enhancements of kynurenine emissions have also been reported in studies of daptomycin interactions with phosphatidylcholine (Lakey and Ptak, 1988).

Kynurenine and tryptophan emissions were slightly blue shifted indicating a change in its local microenvironment for these residues due to interactions between daptomycin and the dendrimer (Figure 15). Typically blue shifts of protein fluorescence are due to shielding of fluorophores from an exposure hydrophilic environment or residing of fluorophores inside hydrophobic microenvironment (Chen, Ludescher and Montville, 1998, Lakowicz, 2006).

The fluorescence spectroscopy is a direct interaction measurement method which does not perturb the interaction. In addition, the observed fluorescence changes could be related to specific fluorophores which provides information on the interaction at a molecular level. As a consequence, the fluorescence spectroscopy appeared to be a suitable technique for the study of interaction between daptomycin and dendrimer and further determination of the binding parameters

2.3.2 Determination of concentration range

Fluorescence is very sensitive technique; therefore, the appropriate working concentration range was identified by varying the daptomycin concentrations between 3 μM and 1 μM. The titrations were conducted by adding 5 μL aliquots of 82.2 μM PAMAM dendrimer into daptomycin solutions or control solutions. PAMAM generation 5 and phosphate buffer solutions in the absence of daptomycin did not show significant fluorescence emission maxima over the working emission wavelength (320 to 540 nm). Quenching of tryptophan fluorescence intensity and enhancement of kynurenine fluorescence intensity with slight blue-shifting emission peaks for both

tryptophan and kynurenine were seen after the addition of PAMAM generation 5 to the aqueous solution of daptomycin (Figure 16).

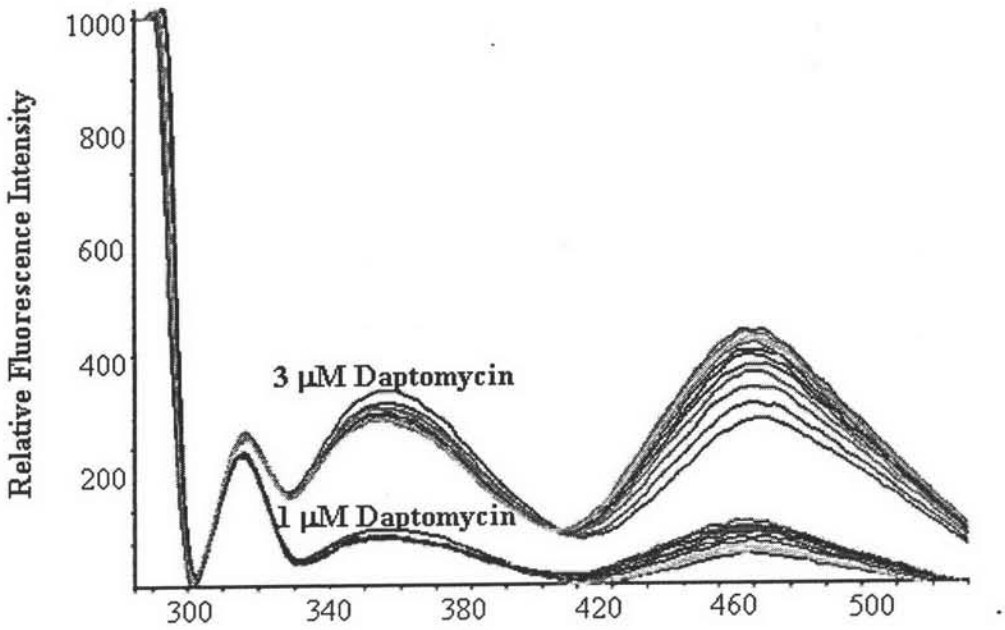

Figure 16 Fluorescence emission spectra obtained from the titration of 1 and 3 μM daptomycin with PAMAM generation 5 by excitation 285 nm and setting excitation/emission slit width 4/15.

The fluorescence intensity obtained from the titration of daptomycin at both concentrations (1 and 3 μM) were within the detection limits. Therefore, the increased fluorescence response observed with 3 μM daptomycin solutions suggested the higher proper concentration to be the most appropriate for further studies. In order to optimize appropriate range of observed fluorescence intensity, the excitation and emission slit widths were varied. Changing the slit width to 6/12 showed the optimum sensitivity in both tryptophan and kynurenine (Figure 17). Thereupon, the concentration of daptomycin and the slit width used in subsequent studies was fixed at 3 μM and 6/12, respectively.

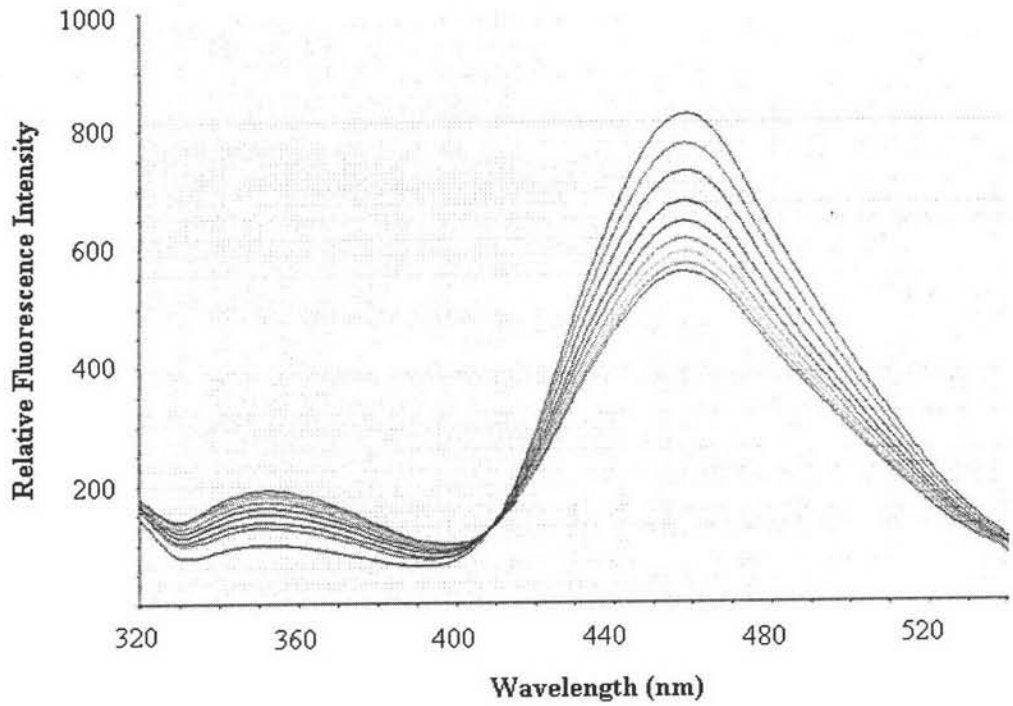

Figure 17 Fluorescence emission spectra obtained from the titration of 3 μM daptomycin with PAMAM generation 5 by excitation 285 nm and setting excitation/emission slit width at 6/12

3. Investigation of pH Effect on the Binding

Ionic interactions between daptomycin and dendrimer were predicted to be the major force in daptomycin-dendrimer complex formation. Thus, factors affecting ionization states of both compounds were investigated.

3.1. The effect of pH on daptomycin-dendrimer complex formation

3.1.1 Titration of PAMAM dendrimer to daptomycin solution at various pH values

The titrations of daptomycin solutions with PAMAM dendrimer generation 5 were conducted over the pH range of 3 to 8 without buffer. The pH value of the system was kept constant by adjusting the pH value of all solutions to the desired pH value before adding them together. Titration were conducted by incrementally adding dendrimer to fixed concentrations of daptomycin or conversely by adding daptomycin to dendrimer. For the former type of titration, the daptomycin solution was placed in a fluorescence cuvette, and 5 μL aliquots of 73.1 μM PAMAM dendrimer were incrementally added. The pH value remained essentially constant (Δ pH < 0.1).

The fluorescence intensities of daptomycin solutions (in the absence of dendrimer) were determined as a function of pH in the range of interest. Comparison of the fluorescence intensity values over the entire pH range (Table 6 and Table 7) failed to yield any statistically significant differences at the $p = 0.05$ level (ANOVA using SPSS software version 16.0; SPSS Inc, Chicago, IL).

Table 6 The fluorescence emission intensity at 355 and 460 nm of 3 μM daptomycin in the pH range 3 to 8

	Fluorescence emission intensity			
	at 355 nm		at 460 nm	
pH	Average	SD	Average	SD
3	148.33	0.17	105.33	1.37
4	128.01	18.36	95.41	24.79
5	128.74	9.24	107.04	11.19
6	117.72	0.35	108.17	0.40
7	127.80	2.91	117.71	3.46
8	122.72	3.13	114.86	4.58

Table 7 One-way ANOVA analysis of the fluorescence emission spectra from daptomycin solution at various pH values

ANOVA					
	Sum of Squares	df	Mean Square	F	Sig.
Between Groups	1085.593	5	217.119	2.953	.110
Within Groups	441.170	6	73.528		
Total	1526.763	11			

In order to obtain the fluorescence intensity values associated with daptomycin-dendrimer interactions (ΔF), the fluorescence intensities measured after the incremental addition of each dendrimer aliquot was subtracted from that of daptomycin solution at the same concentration. The binding isotherm was constructed by plotting the differences (ΔF) against total daptomycin concentration (Figure 18).

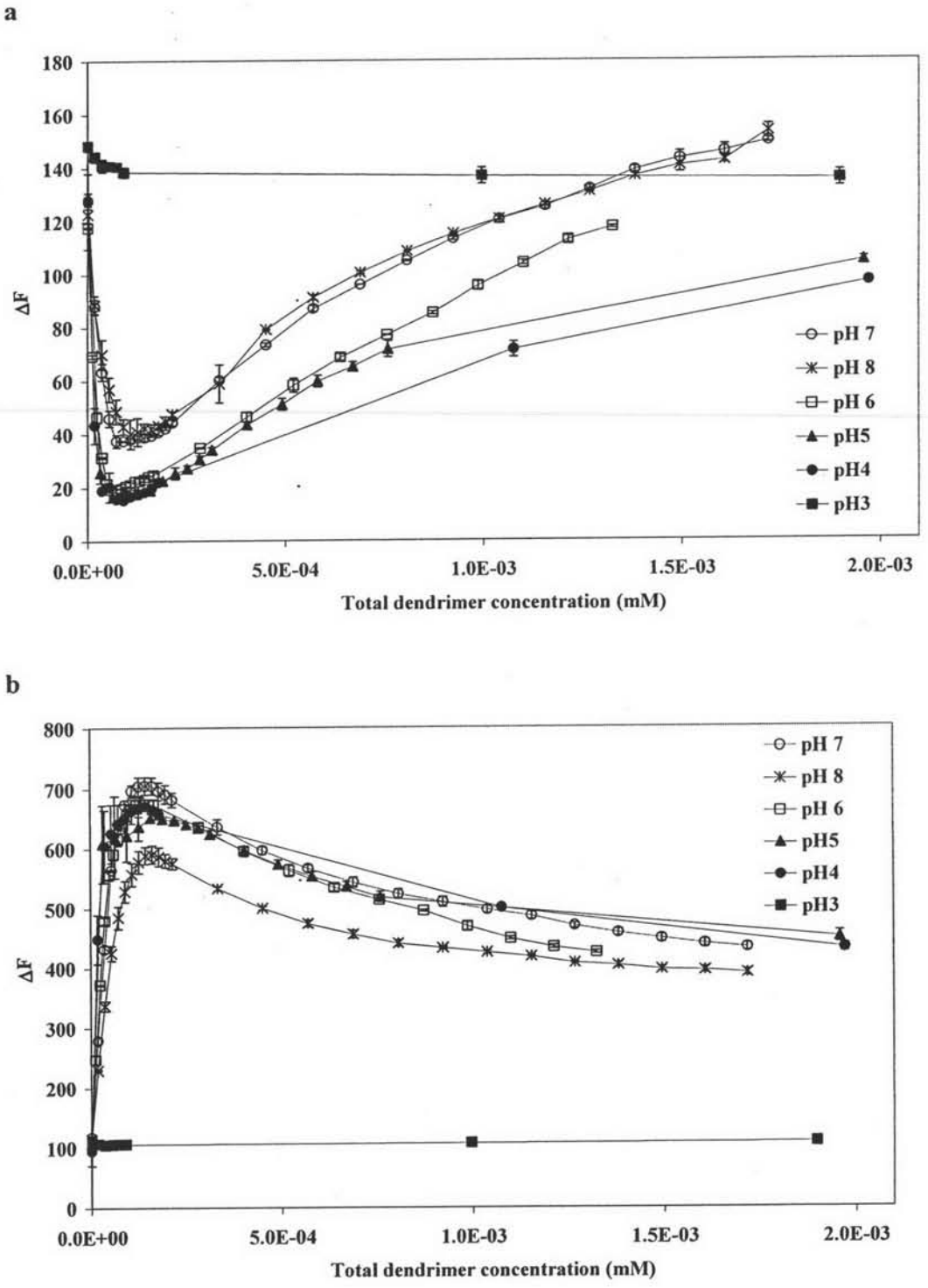

Figure 18 Binding isotherms obtained from the fluorescence emission intensities (a) at 355 nm and (b) at 460 nm of the titration of daptomycin solution with PAMAM dendrimer generation 5 at various pH

The shape of binding isotherms obtained at 355nm from the titration of daptomycin solution with PAMAM dendrimer generation 5 was used to deduce the nature of binding processes. Under the conditions reported herein, the shapes of the isotherms were similar regardless of pH values, excepting for the binding isotherm at pH 3 (Figure 18a). At pH 3, the ΔF decreased with the initial additions of PAMAM dendrimer and remained constant with the addition of PAMAM dendrimer aliquots. Contrariwise, in the pH range of 4 to 7, the isotherms showed a sharp decrease in ΔF at low concentration of dendrimer, minimum at total a PAMAM dendrimer concentration about 7.26×10^{-5} mM and an increase as PAMAM dendrimer was subsequently added to the reaction mixture.

The corollary plots of ΔF versus total dendrimer concentration at an emission wavelength of 460 nm were nearly mirror images of the binding isotherm obtained at 355 nm (Figure 18). However at pH 3, ΔF was independent of PAMAM dendrimer concentration. In the pH range of 4 to 7, ΔF sharply increased in the presence of PAMAM dendrimer, reached a maximum in the range of 0.75 to 1.44×10^{-4} mM PAMAM, and then decreased gradually with increasing dendrimer concentration.

Daptomycin-dendrimer interactions appeared to affect the fluorescent properties of both tryptophan and kynurenine based on the observation that the emissions at both 355 and 460 nm were altered in corollary manner. This observation suggests that microenvironments of both fluorophores were affected by the intermolecular interactions.

In addition, the shapes of the binding isotherms in the pH range of 4 to 8 were biphasic suggesting that two processes were involved in the daptomycin-dendrimer interactions. In the presence of excess daptomycin and relatively low dendrimer concentrations, the isotherm shapes suggest a relatively high affinity binding event causing a precipitous change in the fluorescence intensity responses.

The addition of excess dendrimer appeared to cause a denegation of the daptomycin fluorescence response as manifested by a gradual decrease in tryptophan quenching at 355 nm corresponding a decrease in kynurenine emission at 460 nm. Moreover, the rate of loss of tryptophan quenching or kynurenine emission with respect to increasing dendrimer concentration was more rapid at higher pH values (6 – 8) then at pH values of 4 to 5. This observation suggests that as the anionic charge on daptomycin

was increased the denegation of the fluorescence changes associated with binding was greater. Taken together these observations suggest that in the presence of excess dendrimer some loss of binding occurs perhaps due to the "shared" interactions of individual daptomycin molecules with more than one dendrimer molecules. Or the changes could be due to conformation changes caused by the distribution of anionic charge in the presence of massive cationic species. The same type of fluorescence change has been previously observed under conditions were the ester bond forming the cyclic peptide structure was hydrolyzed (Muangsiri and Kirsch, 2001). In that situation, the fluorescence changes were attributed to structural changes causing increased separation of the two fluorophores and a decrease in energy transfer between tryptophan and kynurenine.

3.1.2. Titration of daptomycin to PAMAM dendrimer solution at various pH values

In addition to conducting titrations by incrementally adding dendrimer to fixed concentrations of daptomycin, experiments were also conducted by adding daptomycin to dendrimer. This experimental design was expected to yield more useful and typical binding isotherms wherein the ligand concentration is gradually increased in the presence of a fixed substrate concentration. Titrations of daptomycin to dendrimer were conducted over the pH ranging from 3 to 9 without using buffer system. Again all solutions were pH-adjusted to the desire value prior to their addition to one another, and again as before, the pH values of the mixtures did not significantly change. Only minor changes in fluorescence intensity as a function of increasing daptomycin concentration was observed at 355 nm, whereas large enhancements of fluorescence response (over that observed in the absence of PAMAM) were observed at 460 nm. As a consequence, only the 460 nm data were used to develop the binding model and estimate binding parameters.

Typical fluorescence changes as a function of daptomycin concentration are depicted in Figure 19. In the absence of PAMAM, fluorescence intensity increased linearly with daptomycin concentration at all pH values and the increases were essentially co-linear (Table 17, Appendix B). In the presence of PAMAM, fluorescence increases due to the incremental addition of daptomycin were not linear and were different over the pH range studied (Figure 19). Typically, most of daptomycin

titration profiles displayed a steep fluorescence increase at low daptomycin concentration of followed by a gradual linear increase at higher concentrations.

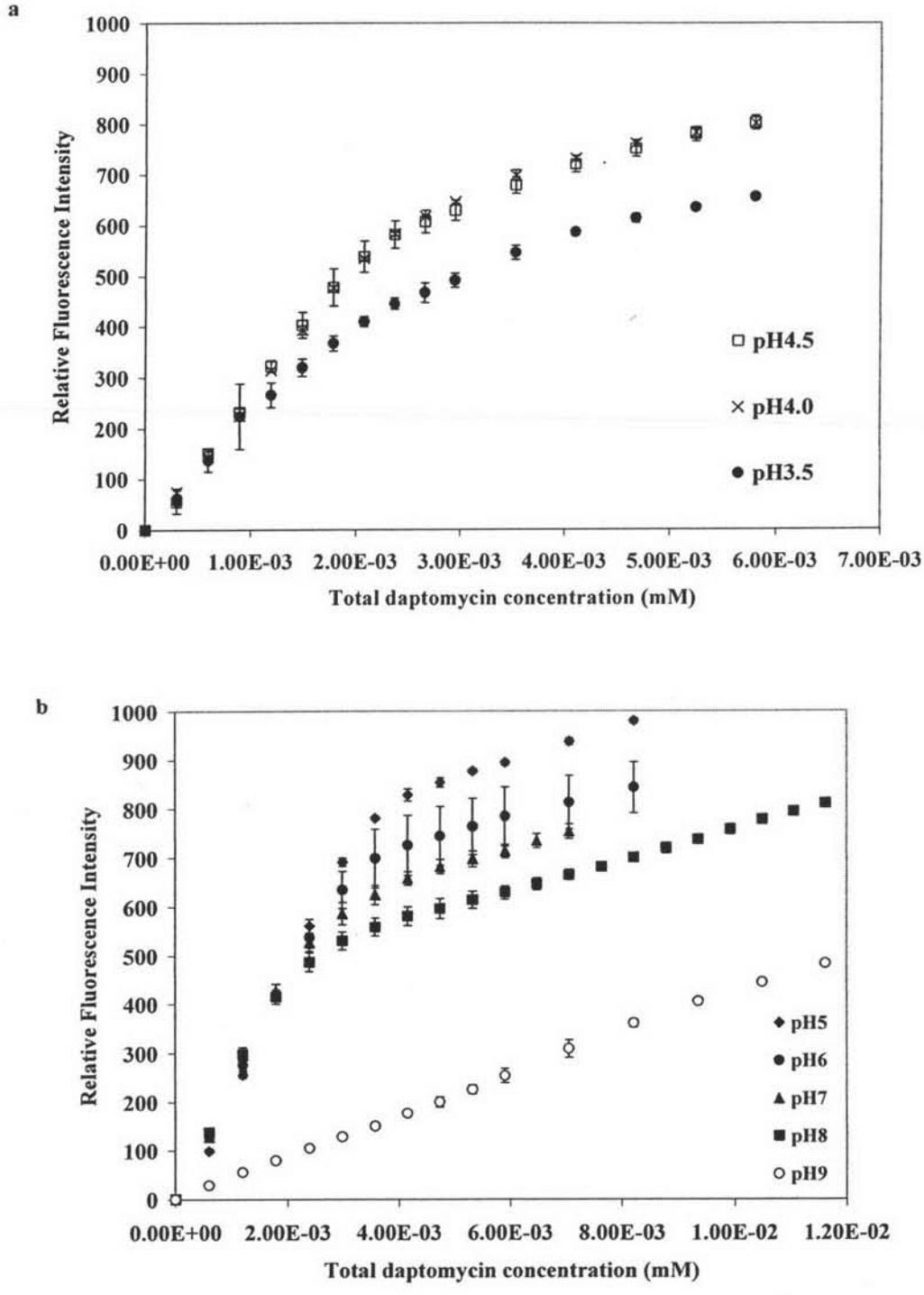

Figure 19 Kynurenine fluorescence enhancement of daptomycin at 460 nm obtained from the titration of PAMAM dendrimer generation 5 solution with daptomycin. (a) 0.05 μM PAMAM generation 5 at pH range of 3.5, 4 and 4.5 and (b) 0.27 μM PAMAM generation 5 at pH range of 3, 5, 6, 7, 8 and 9

The fluorescence intensity of mixtures of daptomycin and dendrimer was a result of the sum of fluorescence emissions from both free daptomycin and the daptomycin-dendrimer complexes. The enhancement in emission intensity at low concentrations of daptomycin (over that observed in the absence of dendrimer) was likely due to the complex formation. The gradual increase in the fluorescence intensity was found observed at higher daptomycin concentration appeared to parallel the increases observed in the absence of dendrimer and was initially believed to be due increased concentrations of free daptomycin in the presence of saturated dendrimer-daptomycin complexes (Figure 20). But a detailed, careful analysis of binding isotherms will be further discussed.

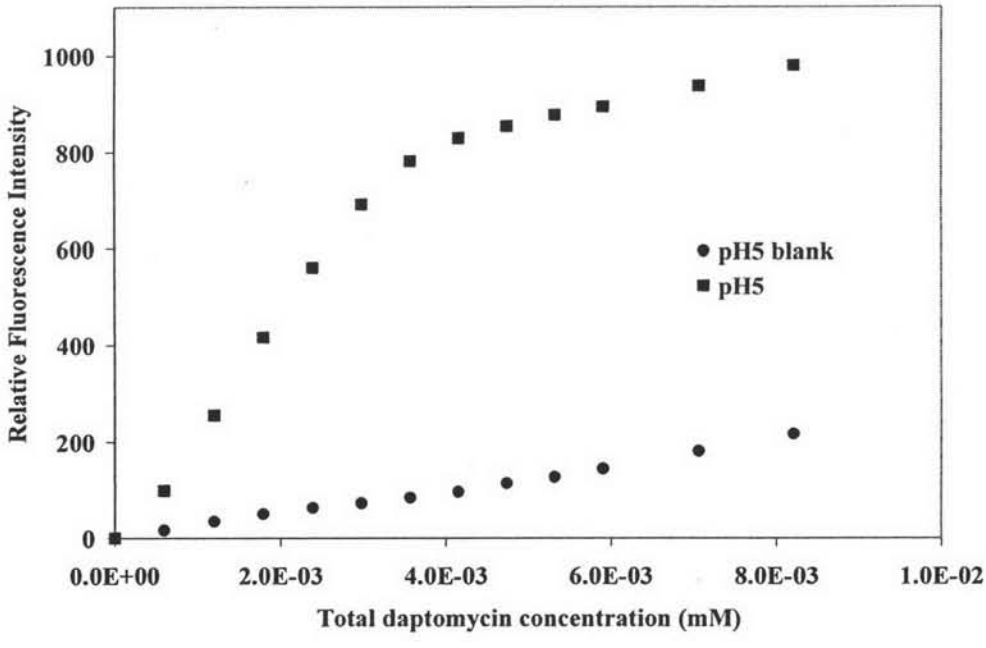

Figure 20 Comparison of the daptomycin fluorescence enhancement at 460 nm obtained from the titration at the presence and absence of PAMAM dendrimer generation 5 at pH 5

3.1.3. Binding isotherm construction

The significant difference in fluorescence intensity (ΔF) of daptomycin in the presence versus the absence of dendrimer indicated an interaction between dendrimer and daptomycin. The binding isotherm was constructed by plotting the difference between the fluorescence intensity in the presence and absence of

dendrimer (ΔF) against the total daptomycin concentration. The magnitudes of the ΔF increases in the pH range of 3.5 to 4.5 were very dramatic and exceeded the detection limit of the spectrometer (data not shown). Hence, the dendrimer concentration reactions in this pH range were lowered to 0.05 μM and the daptomycin aliquots were decreased in a corresponding manner. The magnitude of the enhancement suggested that very significant binding occurred in the 3.5 to 4.5 pH region. In order to compare all of the isotherm obtained at different pH values using different dendrimer concentrations, the data were normalized by dividing the observed ΔF values by the total dendrimer concentration (Figure 21).

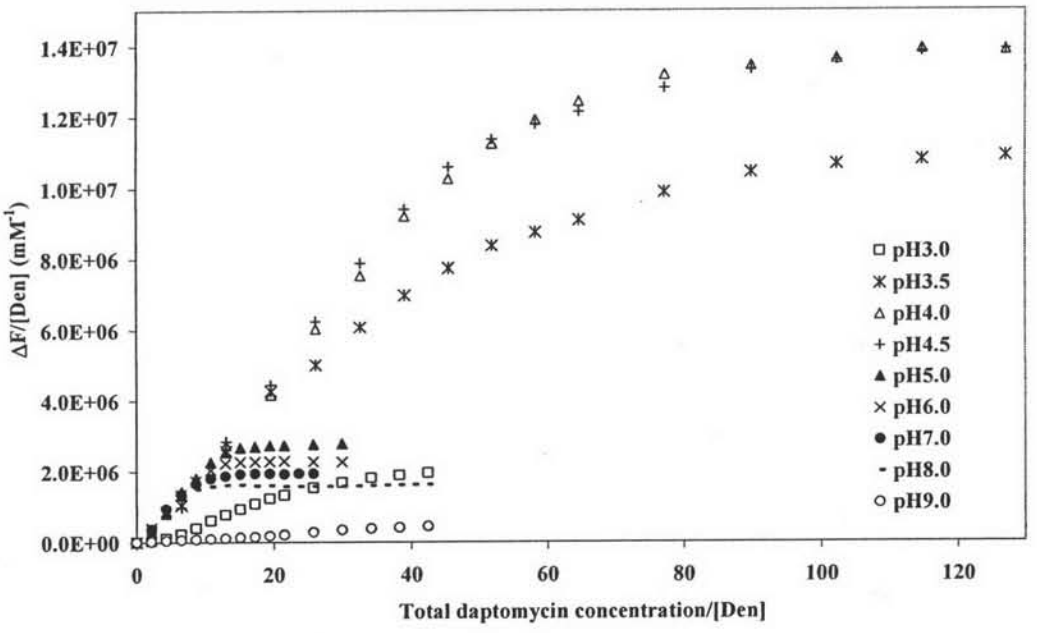

Figure 21 The binding isotherm of the interaction between PAMAM generation 5 and daptomycin at different pH ranging from 3.0 to 9.0

The shapes of the isotherms were used to deduce the nature of the binding process and then used to estimate the binding parameters, dissociation constant (K_d) and the total number of independent binding sites (R) by fitting appropriate model equations to the experimental data using nonlinear regression methods. A detailed discussion of the effects of binding parameter values on the shapes of the isotherms and

the identification of initial values for binding constants (later used to accurately estimate the constant values by nonlinear regression) is provided in Section 4.4.

Typically the binding isotherms shapes were similar at different pH values except at pH 3 and pH 9. Typical isotherms (pH 4 to 8) showed a steep increase at low concentration of daptomycin and a plateau at higher concentrations of daptomycin. The plateau region suggested binding saturation. Taken together the isotherms suggested a single site binding model.

The isotherms at pH 3 showed sigmoidal shape with an initial lag phase at low concentration of daptomycin, followed by a hyperbolic phase. At the pH 3, approximately fifty percent of the daptomycin molecules are in a cationic form and the rest are in zwitterionic. Cationic daptomycin would not be expected to interaction with cationic dendrimer due to electrostatic repulsion. Zwitterionic daptomycin appeared to effectively bind dendrimer. Therefore, the lag phase would appear to reflect the decreased ability of daptomycin to bind dendrimer due to the presence of unfavorable ionic forms at low pH values.

At pH 9.0, the different fluorescence intensity gradually increased with increased daptomycin concentration and did not reach a plateau. At this pH, about half of interior amines in PAMAM (tertiary amines with pKa of 6.3 to 7.2) were deprotonated. Thus the total positive charge of PAMAM was reduced. Moreover, the loss of interior positive charge causes the molecular structure of PAMAM dendrimers to collapse (Maiti et al., 2005). Likely this collapse reduced the dendrimer radius of gyration and surface area. In short at pH 9, PAMAM dendrimers and daptomycin do not appear to form effectively complex.

3.2. The effect of pH on the binding parameters

3.2.1. The estimation of the binding parameters; molar signal coefficient (ΔF), dissociation Constant (K_d) and capacity constant (n)

3.2.1.1. Mathematical model; one site binding model

The shape of the binding isotherms suggested that a one site binding model could be used to adequately describe the interaction of daptomycin and 5th generation PAMAM dendrimers in the pH region 3.5 to 8. In this model, ligand

reversibly binding to a single type of binding sites on the substrate. Thus a thermodynamic equilibrium between dendrimer, daptomycin and the complex can be described as:

$$[\text{Den}] + [\text{Dap}] \underset{}{\overset{K}{\rightleftharpoons}} [\text{Den - Dap}]$$

$$K = \frac{[\text{Den - Dap}]}{[\text{Den}]\times[\text{Dap}]}$$

where [Den], [Dap] and [Den-Dap] represented concentration of free dendrimer, free daptomycin, and complex respectively. The equilibrium constant, K, is defined as the association constant and the dissociation constant (K_d) is the simply inverse of K_a is given by

$$K_d = \frac{[\text{Den}]\times[\text{Dap}]}{[\text{Den - Dap}]} \qquad \text{equation 15}$$

Based on the mass balance, equation 15 can be rearranged to equation 16

$$K_d = \frac{([\text{Den}]_T - [\text{Den - Dap}])\times[\text{Dap}]}{[\text{Den - Dap}]} \qquad \text{equation 16}$$

where $[\text{Den}]_T$ is total dendrimer concentration. The fraction of bound ligand, r, is the moles of daptomycin bound ([Den-Dap]) per mole of total dendrimer ($[\text{Den}]_T$); then equation 16 became

$$r = \frac{[\text{Dap}]}{K_d + [\text{Dap}]} \qquad \text{equation 17}$$

The term, n, represents the number of independent binding sites are available on the dendrimer, thus the fraction of bound ligand per mole of dendrimer is given by

$$r = \frac{n\times[\text{Dap}]}{K_d + [\text{Dap}]}$$

Let R be the total number of independent binding sites; then

$$[\text{Den - Dap}] = \frac{R\times[\text{Dap}]}{K_d + [\text{Dap}]}$$

Because the change in fluorimetric signal (ΔF) is directly proportional to complex concentration, the normalized change in fluorescence intensity is given by

$$\Delta F = \Delta E\times[\text{Den - Dap}] = \Delta E\times\frac{R\times[\text{Dap}]}{K_d + [\text{Dap}]} \qquad \text{equation 18}$$

where constant ΔE is a proportional constant corresponding to the different in signal changes (ΔF) per unit complex or molar signal coefficient.

According to equation 18, the free daptomycin is needed in order to estimate binding constants. But equation 18 can be modified in terms of total ligand concentration by invoking mass balance constraints:

$$[\text{Den - Dap}] = \frac{R \times ([\text{Dap}]_T - [\text{Den - Dap}])}{K_d + ([\text{Dap}]_T - [\text{Den - Dap}])} \quad \text{equation 19}$$

Equation 19 can be rearranged into a quadratic expression

$$[\text{Den - Dap}]^2 - (R + Kd + [\text{Dap}]_T) \times [\text{Den - Dap}] + R \times [\text{Dap}]_T = 0 \quad \text{equation 20}$$

wherein the roots of quadratic equation, equation 20, are

$$[\text{Den - Dap}] = \frac{1}{2}\{([\text{Den}]_T + K_d + R) \pm \sqrt{([\text{Den}]_T + K_d + R)^2 - 4 \times R \times [\text{Dap}]_T}\} \quad \text{equation 21}$$

Substitution of equation 21 into equation 18 yields

$$\Delta F = \frac{\Delta E}{2}\left\{([\text{Den}]_T + K_d + R) \pm \sqrt{([\text{Den}]_T + K_d + R)^2 - 4 \times R \times [\text{Dap}]_T}\right\} \quad \text{equation 22}$$

The equation 22 was described by a hyperbolic relationship between the change in fluorimetric signal (ΔF) and total daptomycin concentration ($[\text{Dap}]_T$). The form value is experimentally determined and the latter is known thus curve fitting this model equation to the experimental data results in estimates for the model constants including the molar signal coefficient (ΔE), the dissociation constant (K_d) and the total number of independent binding sites (R).

3.2.1.2. Fitting of model parameters to experimental data

The binding parameters were estimated by fitting the model equation (22) to the binding isotherm by nonlinear regression analysis using WinNonlin (v 7, Pharsight). Typical curve fitting appeared to completely describe the experiment data (Figure 45 to 47, Appendix C). For example, the predicted curve corresponded to the observed binding isotherm obtained from PAMAM generation 5 with daptomycin at pH 7 (Figure 22). In addition, the residual plots did not show regions of systematic bias (Figure 22b).

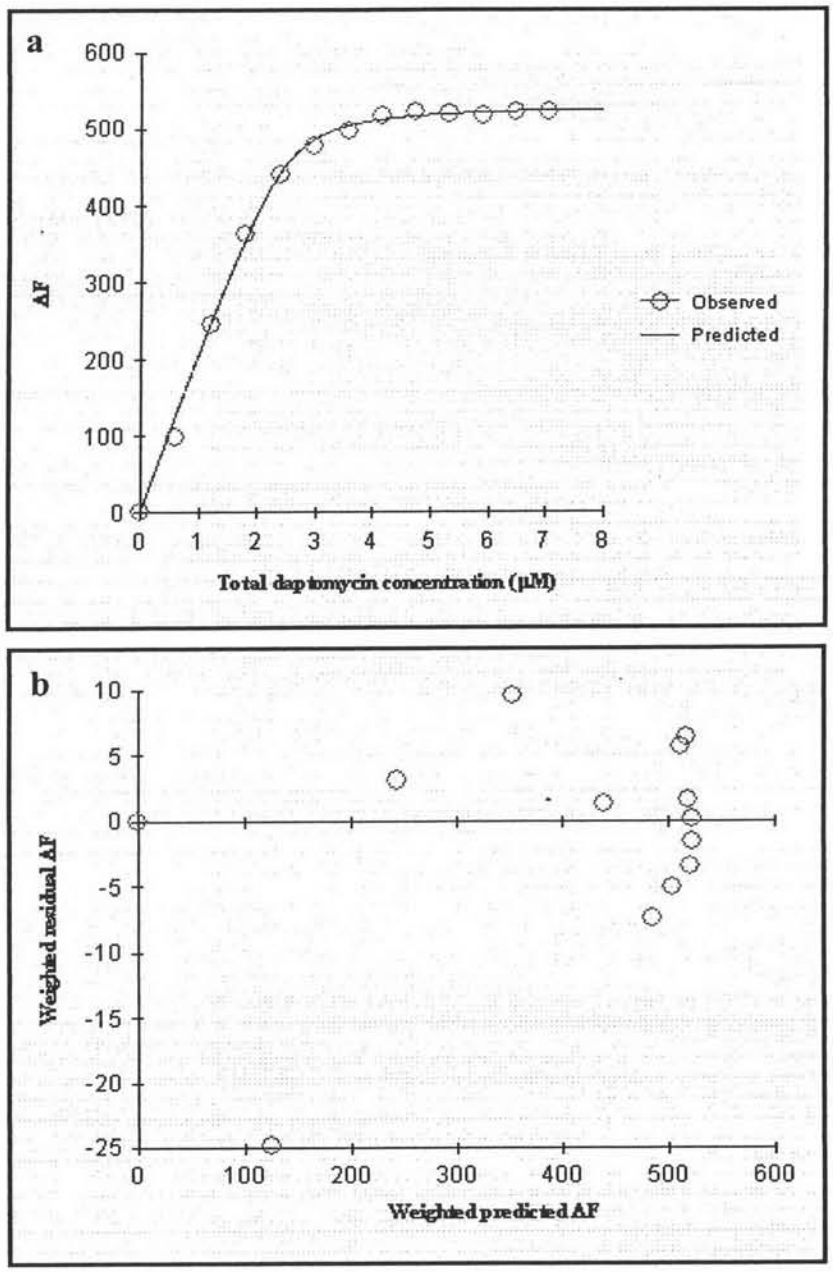

Figure 22 (a) Binding isotherm obtained from the interaction between PAMAM generation 5 and daptomycin at pH7.0 and 25°C (opened circle) and fitting curve (solid line) and (b) residuals plot of weighted residual ΔF against weighted predicted ΔF

The molar signal coefficient (ΔE), the dissociation constant (K_d) and the number of independent binding sites (R) were estimated at each pH value except at pH 3 and 9 were binding appeared to be marginal or non-existent. Dividing the

estimated R values by total concentration of dendrimers provided the capacity constant (n). The binding parameters were reported in Table 8.

Table 8 Table show estimate values of the molar signal coefficient (ΔE), dissociation constant (K_d; μM^{-1}), the binding capacity (n; molecules of daptomycin per one molecule of PAMAM dendrimer) at various pH ranges of the binding interaction between daptomycin and PAMAM denrimer generation 5 (replications = 2)

	Binding parameters						
	ΔE		K_d (μM^{-1})		n		
pH	Average	SD	Average	SD	Average	SD	Model
3.5	227.56	31.73	0.26	0.02	47.18	6.18	1-type
4	244.30	2.43	0.07	0.00	52.89	1.34	1-type
4.5	259.35	13.23	0.10	0.02	49.89	1.99	1-type
5	207.15	5.81	0.01	0.00	13.54	2.63	1-type
6	205.20	4.63	0.02	0.01	11.39	4.06	1-type
7	219.27	9.18	0.06	0.01	9.14	0.80	1-type
8	216.94	11.54	0.03	0.03	7.58	3.08	1-type

The molar signal coefficient (ΔE) obtained from the fitting of binding isotherms at pH ranges of 3.5 to 8 were not significantly different (p-value = 0.053) (Table 18, Appendix B). The constant value of ΔE indicated that the fluorescence characteristics of the interaction between daptomycin and PAMAM dendrimer generation 5 was identical throughout the pH range of 3.5 to 8. Consequently ΔE value was fixed for all binding isotherms at a constant mean value of 225.68. Then Equation 22 was re-fit to all binding isotherms with just two adjustable parameters in an attempt to attribute pH differences to the binding parameters, K_d and R. The results are presented in Figure 48 to 50 (Appendix C). The capacity constant (n) of each individual pH value was calculated based on estimated R value and total concentration of PAMAM dendrimer. The re-estimated binding parameters were reported in Table 9. The capacity constant appeared to change dramatically as a function of pH. In addition, the one-way ANOVA and Post Hoc analysis of K_d showed that the estimated K_d obtained from the binding isotherm at pH 3.5 was significantly higher than the others (p-value = 0.002) (Table 19, Appendix B).

At pH 3.5, approximately thirty percent of daptomycin are in cationic forms which are not preferable to form a complex. Therefore, the higher K_d or the lower affinity was suspected to cause by the interfering of cationic daptomycin species in the system.

Table 9 Table show estimate values of dissociation constant (K_d; μM^{-1}) and capacity constant (n; molecules of daptomycin per one molecule of PAMAM dendrimer) at various pH ranges of the binding interaction between daptomycin and PAMAM dendrimer generation 5 analyzed by fixing the molar signal coefficient (ΔE) as a constant at 225.68 (replications =2)

	Binding parameters				
	K_d (μM^{-1})		n		
pH	Average	SD	Average	SD	Model
3.5	0.19	0.00	46.28	0.00	1-type
4	0.03	0.00	55.92	0.96	1-type
4.5	0.03	0.03	55.29	0.39	1-type
5	0.07	0.02	12.75	0.23	1-type
6	0.08	0.03	10.58	0.88	1-type
7	0.08	0.03	8.93	0.15	1-type
8	0.04	0.01	7.29	0.19	1-type

3.2.2. Assessment of the relationship between the ionic properties of daptomycin, PAMAM dendrimer and binding capacity

Ionization profiles of daptomycin and dendrimer were constructed based on pKa calculation and compared with the changes in binding capacity (n) in different pH ranges (Figure 23 and 24).

Daptomycin contains six ionizable groups which include four carboxylic acid side chains (three aspartic acids and one methyl-glutamic acid) and two primary amines (kynurenine and ornithine). Preliminary analysis of NMR data (Qiu and Kirsch, unpublished) suggests that asp-3 has a pK_a of 3, and other two aspartic acids and methyl-glutamic acid have overlapping pK_a's about 5.3. Kynurenine and ornithine have pK_a of 0.8 and 10, respectively (Muangsiri and Kirsch, 2001). The fraction of each ionic

species was estimated using the following equations derived from ionization equilibria and mass balance considerations.

$$fH_4P = \frac{1}{\left[1+\left(\frac{Ka_1}{a_H}\right)+\left(\frac{3\times Ka_1\times Ka_2}{a_H^{\,2}}\right)+\left(\frac{3\times Ka_1\times Ka_2\times Ka_3}{a_H^{\,3}}\right)+\left(\frac{Ka_1\times Ka_2\times Ka_3\times Ka_4}{a_H^{\,4}}\right)\right]}$$

$$fH_3P = \frac{1}{\left[1+\left(\frac{a_H}{Ka_1}\right)+\left(\frac{3\times Ka_2}{a_H}\right)+\left(\frac{3\times Ka_2\times Ka_3}{a_H^{\,2}}\right)+\left(\frac{Ka_2\times Ka_3\times Ka_4}{a_H^{\,3}}\right)\right]}$$

$$fH_2P = \frac{3}{\left[3+\left(\frac{a_H^{\,2}}{Ka_1\times Ka_2}\right)+\left(\frac{a_H}{Ka_2}\right)+\left(\frac{3\times Ka_3}{a_H}\right)+\left(\frac{Ka_3\times Ka_4}{a_H^{\,2}}\right)\right]}$$

$$fHP = \frac{3}{\left[3+\left(\frac{a_H^{\,3}}{Ka_1\times Ka_2\times Ka_3}\right)+\left(\frac{a_H^{\,2}}{Ka_2\times Ka_3}\right)+\left(\frac{3\times a_H}{Ka_3}\right)+\left(\frac{Ka_4}{a_H}\right)\right]}$$

$$fP = \frac{1}{\left[1+\left(\frac{a_H^{\,4}}{Ka_1\times Ka_2\times Ka_3\times Ka_4}\right)+\left(\frac{a_H^{\,3}}{Ka_2\times Ka_3\times Ka_4}\right)+\left(\frac{3\times a_H^{\,2}}{Ka_3\times Ka_4}\right)+\left(\frac{3\times a_H}{Ka_4}\right)\right]}$$

where fH_4P, fH_3P, fH_2P, fHP and fP represented the ionic function of cationic, zwitterionic, anionic, dianionic and trianionic species of daptomycin, respectively. The Ka_1 were ionization constant for asp-3, whereas Ka_2, Ka_3 and Ka_4 were overlapping ionization constant of other two aspartic acids and methyl-glutamic acid. The a_H was defined as the activity of hydronium ion related to the pH value.

$$a_H = 10^{-pKa}$$

Substitution of the carboxylic acid pKa values into these equation resulted in the ionization profile of daptomycin (Figure 23). In a pH range of 0.8 to 3, major ionic species of daptomycin is a monocationic form due to the deprotonation of aromatic amine kynurenine. A zwitterionic form dominates in a pH range of 3 to 5 due to the protonation of asp-3. Deprotonation of other three carboxylic acid groups gives rise to monoanionic, dianionic and trianionic forms in a pH range of 5 to 9.

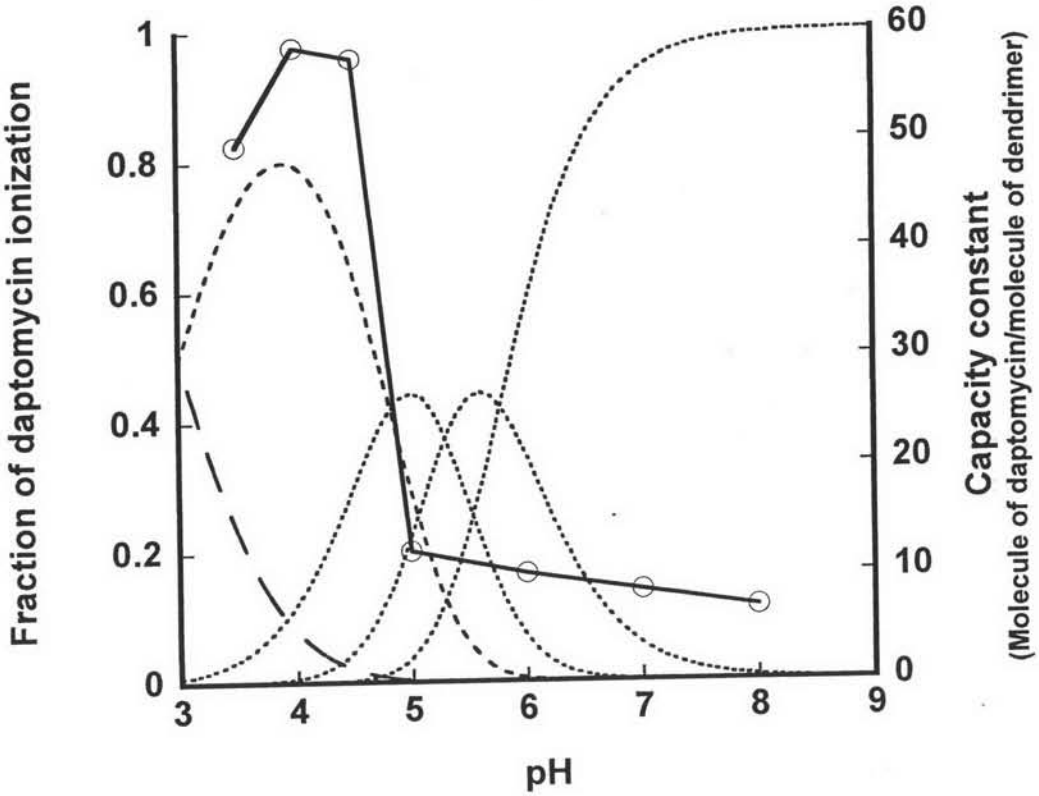

Figure 23 Comparison of species distribution diagram of daptomycin with binding capacity of the interaction between PAMAM generation 5 and daptomycin. Fraction of daptomycin ionization varied from (——) cation, (-·--) zwitterion, (·····) anion, dianion and trianion, respectively. Each point (-⊖-) represented the capacity constant at various pH.

The protonation profile of PAMAM dendrimer generation 5 is depicted in Figure 24 and was based on estimates reported by Diallo et al. (Diallo et al., 2004). PAMAM dendrimer generation 5 possesses two types of cationic amino groups. Each molecule contains 126 interior tertiary amines with pK_a values in the range of 6.3 to 7.2 and 128 surface primary amines with pK_a values in the range of 9.0 to 10.8 (Niu, Sun and Crooks, 2003; Cakara, Kleimann and Borkovec, 2003). PAMAM dendrimer shows positive charges on its surface due to primary amine protonation throughout the experimental pH range, whereas the interior amines gradually deprotonation over the pH range of 5 to 9 (Figure 24).

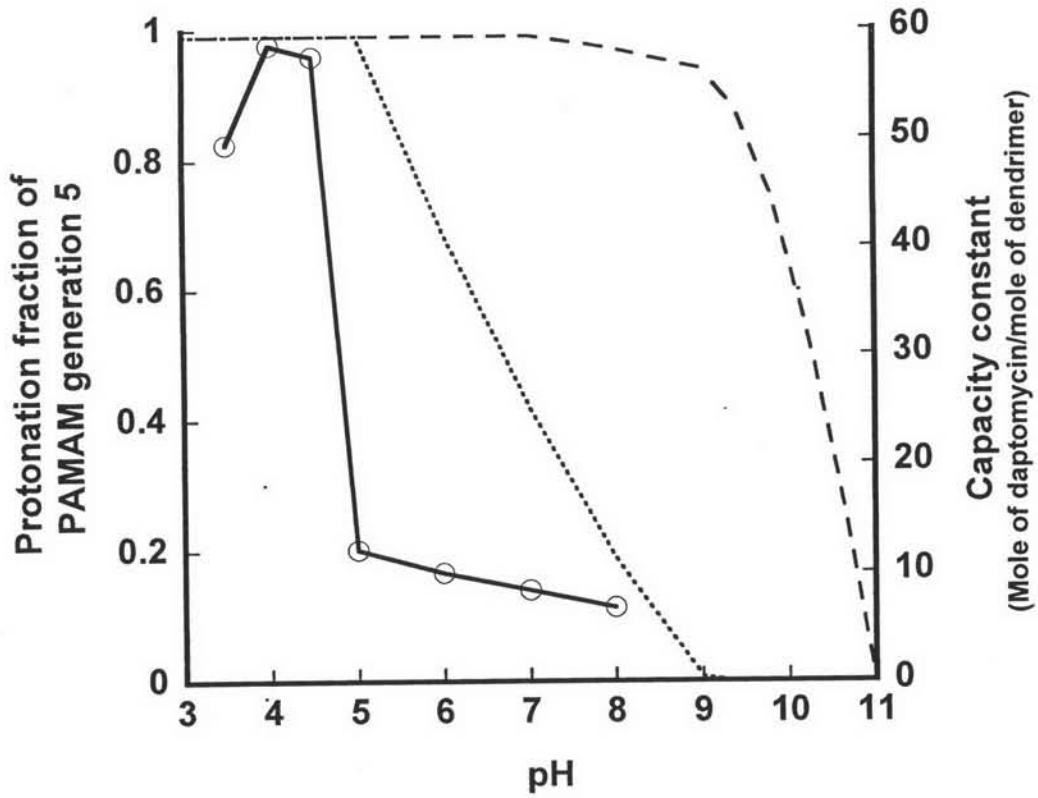

Figure 24 Comparison of protonation profiles of PAMAM generation 5 with binding capacity of the interaction between PAMAM generation 5 and daptomycin. The tertiary amine (·····) gradually deprotonate from pH 5 to pH 9, whereas primary amine (- - -) deprotonate after pH 7. Each point (-⊖-) represented the capacity constant at various pH.

Comparisons of the ionization profiles of the dendrimer and daptomycin to the profile of binding capacity suggest that the primary determinant in the magnitude of the binding capacity is the fraction of zwitterionic form of daptomycin (Figure 23), whereas, only minor changes in the binding capacity can be possibly attributed to the ionic state of the dendrimer (Figure 24). This suggests binding may be due to electrostatic interactions between asp-3 and cationic moieties on the dendrimer surface. Furthermore, these results suggest that additional anionic charges on daptomycin weaken, rather than strengthen, daptomycin-dendrimer interactions. Once daptomycin is electrostatically bound to dendrimer, the remaining cationic residue in daptomycin allows the total charge of the complex to remain unchanged and permits electrostatic attraction of additional daptomycin molecules to the dendrimer surface.

4. Investigation of the effects of dendrimer size on daptomycin-dendrimer interactions

4.1. The effect of dendrimer generation size on complex formation

4.1.1 The effect of PAMAM generation 6 on complex formation

The titrations of daptomycin to dendrimer generation 6 were conducted in the pH range of 3.5 to 7 in the absence of buffers. The concentration of PAMAM dendrimer generation 6 and daptomycin were 0.014 and 74.07 μM, respectively. Titration procedures and construction of binding isotherms were carried out as described for titrations involving dendrimer generation 5. The resultant binding isotherms are depicted in Figure 25.

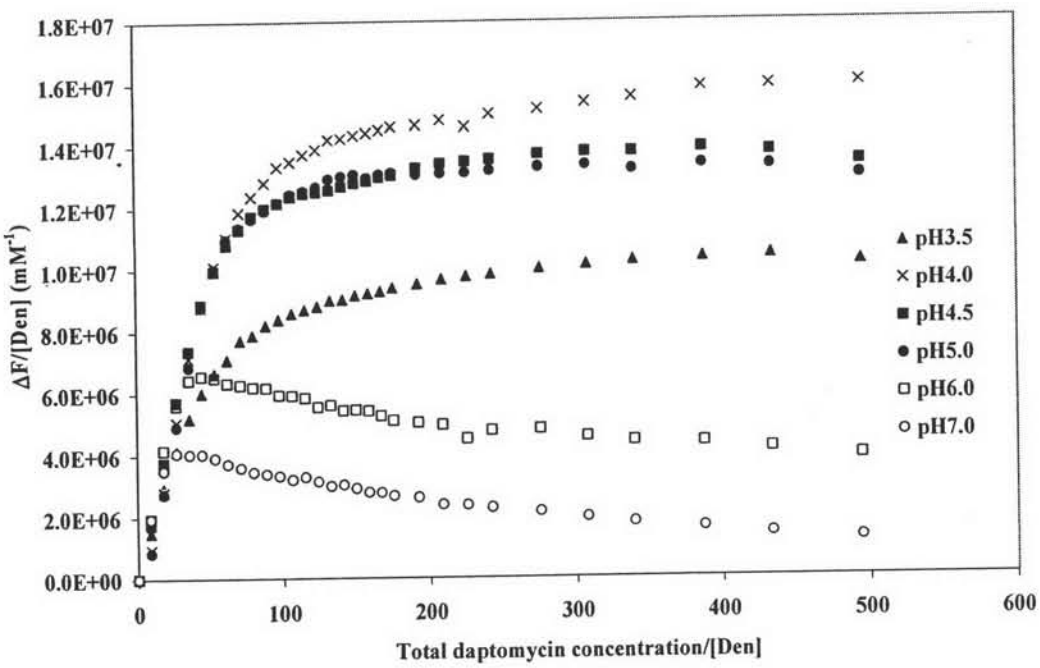

Figure 25 The binding isotherm of the interaction between PAMAM generation 6 and daptomycin at different pH ranging from 3.5 to 7

In these studies, the shapes of the binding isotherms were pH-dependent. In a pH range of pH 3.5 to 5, the differences in fluorescence emission intensity (ΔF) were consistent with the one site binding site model described by titration data generated using dendrimer generation 5. The ΔF values steeply increased and attained plateaus at higher daptomycin concentrations. In the pH range of 6 to 7, the isotherm were different in that the ΔF values increased at low daptomycin concentration, attained a maximum value and then gradually decreased with increasing in daptomycin concentrations. This isotherm shape suggested change in binding at higher concentrations either due to a loss in binding capacity or a second binding site that was associated with a loss in fluorescence intensity.

4.1.2 The effect of PAMAM generation 3 on complex formation

The titrations of dendrimer generation 3 were conducted at the pH of 4 and 7. The concentration of PAMAM dendrimer generation 6 and daptomycin were 0.136 and 74.07 μM, respectively. Again procedures and data transformations were the same as previously described. The resultant binding isotherms are depicted in Figure 26. At pH 4 the binding isotherm shape appeared to be consistent with one site binding model, whereas the binding isotherm at pH 7 was consistent with a two site model. However, a little initial lag phase was observed from the one site binding isotherm at pH 4. This may be a consequence of asymmetry structure of PAMAM generation 3 (Tomalia and Frechet, 2002).

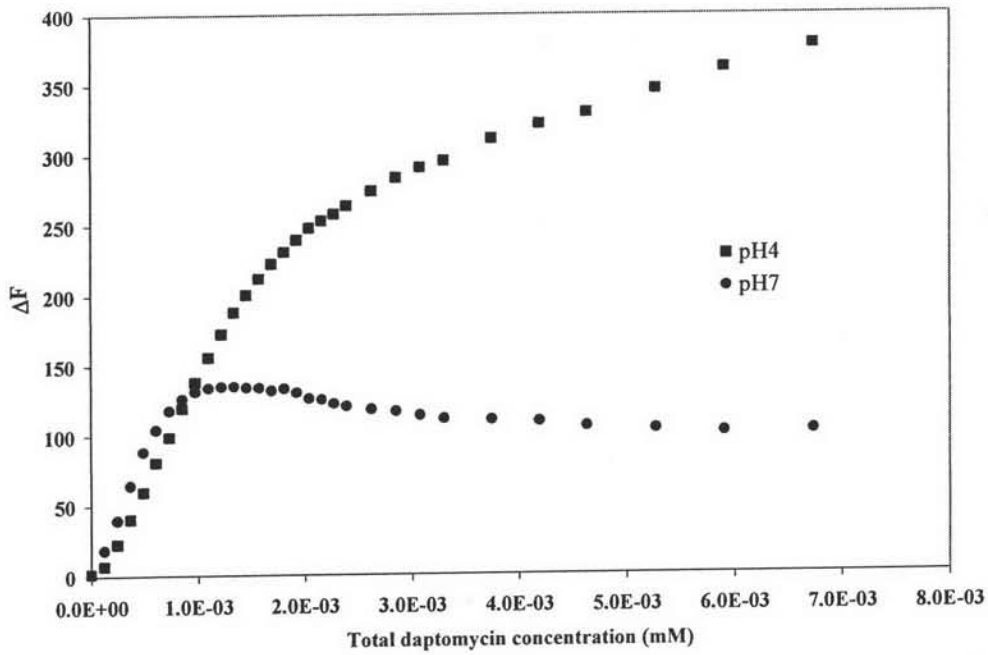

Figure 26 The binding isotherm of the interaction between PAMAM generation 3 and daptomycin at different pH values of 4 and 7

4.2. The effect of generation size on the binding parameters

4.2.1. The estimation of molar signal coefficient (ΔE), dissociation Constant (K_d) and capacity constant (n)

4.2.1.1. Mathematical model; one site binding model and two site binding model

4.2.1.1.1. One site binding model

For those isotherms that were consistent with a one-site model the procedures used to estimate binding parameters were the same as described of dendrimer generation 5 data. Equation 22 was used as described above.

4.2.1.1.2. Two site binding model

Two site binding model is defined for the system wherein ligand interacts with two independent non-interacting binding sites. Then, the concentration of bound molecules, [Den-Dap], is given by

$$[\text{Den - Dap}] = \frac{R_1 \times [\text{Dap}]}{K_{d1} + [\text{Dap}]} + \frac{R_2 \times [\text{Dap}]}{K_{d2} + [\text{Dap}]} \quad \text{equation 23}$$

Where [Dap] is free daptomycin concentration, K_{d1}, R_1 and K_{d2} R_2 are the dissociation constants and the binding capacity for classes 1 and 2, respectively.

Substitution of the mass conservation equation, [Den-Dap] = $[\text{Dap}]_T$ - [Dap], into equation 23 and rearrangement yields

$$[\text{Dap}]^3 - a[\text{Dap}]^2 + b[\text{Dap}] + c = 0 \quad \text{equation 24}$$

where

$$a = K_{d1} + K_{d2} + R_1 + R_2 - [\text{Dap}]_T$$

$$b = K_{d1}K_{d2} + K_{d2}R_1 + K_{d1}R_2 + (K_{d1} + K_{d2})[\text{Dap}]_T$$

$$c = K_{d1}K_{d2}[\text{Dap}]_T$$

Let [Dap] = u-(a/3), equation 24 is transformed to

$$u^3 - \left(\frac{a^2}{3} - b\right) \times u^2 + \left(\frac{2}{27} \times a^3 - \frac{1}{3} \times a \times b + c\right) = 0 \quad \text{equation 25}$$

Since $\Delta < 0$, the three real roots of equation 25 are given by

$$u_1 = \frac{2}{3}\sqrt{(a^2 - 3b)}\cos\frac{\theta}{3}$$

$$u_2 = \frac{2}{3}\sqrt{(a^2 - 3b)}\cos\frac{2\pi - \theta}{3}$$

$$u_3 = \frac{2}{3}\sqrt{(a^2 - 3b)}\cos\frac{2\pi + \theta}{3}$$

where

$$\theta = \arccos\frac{-2a^3 + 9ab - 27c}{2\sqrt{(a^2 - 3b)^3}} \qquad (0 < \theta < \pi)$$

According to the definition of u and the physical conditions of the problem proposed, it can be verified that u_1 express physically meaningful root of equation 25, and u_2 and u_3 were meaningless values. Thus, the physically meaningful root of equation 25 can be written as

$$[\text{Dap}] = -\frac{a}{3} + \frac{2}{3}\sqrt{(a^2 - 3b)}\cos\frac{\theta}{3} \qquad \text{equation 26}$$

If $f_a = 2\sqrt{(a^2 - 3b)}\cos\frac{\theta}{3} - \frac{a}{3}$, equation 26 is transformed to

$$[\text{Dap}] = \frac{1}{3} \times f_a \qquad \text{equation 27}$$

Substitution of equation 27 into equation 23 yields

$$[\text{Den - Dap}] = \frac{R_1 \times f_a}{3K_{d1} + f_a} + \frac{R_2 \times f_a}{3K_{d2} + f_a} \qquad \text{equation 28}$$

Fluorescence intensity is directly proportional to the concentration of fluorophores or

$$F_{Dap} = E_{Dap} \times [\text{Dap}]_T = E_{Dap} \times ([\text{Dap}] + [\text{Den - Dap}]_1 + [\text{Den - Dap}]_2) \qquad \text{equation 29}$$

where $[\text{Den-Dap}]_1$ and $[\text{Den-Dap}]_2$ represents complex concentration of first binding site and second binding site, respectively.

$$F = E_{Dap} \times [\text{Dap}] + E_1 \times [\text{Den - Dap}]_1 + E_2 \times [\text{Den - Dap}]_2 \qquad \text{equation 30}$$

Subtraction of equation 30 with equation 29 gives

$$F - F_{Dap} = \Delta F = \Delta E_1 \times [\text{Den - Dap}]_1 + \Delta E_2 \times [\text{Den - Dap}]_2 \qquad \text{equation 31}$$

where $\Delta E_1 = E_1 - E_{Dap}$ and $\Delta E_2 = E_2 - E_{Dap}$. Substitution of equation 28 to equation 29 yields

$$\Delta F = \Delta E_1 \times \left(\frac{R_1 \times f_a}{3K_{d1} + f_a}\right) + \Delta E_2 \times \left(\frac{R_2 \times f_a}{3K_{d2} + f_a}\right) \qquad \text{equation 32}$$

The equation 32 is derived based on two type binding which two different types of sites are independent to each other. The equation describe biphasic function between the change in fluorimetric signal (ΔF) and total daptomycin concentration ($[\text{Dap}]_T$). Both of these variables are able to obtain from the fluorescence titration. The curve fitting results in three constant values including molar signal coefficient (ΔE), dissociation constant (K_d) and the total number of independent binding sites (R) of each type of binding site.

4.2.1.2. Fitting of model parameters to experimental data

The one site binding isotherms obtained from the titration of dendrimer generation 6 with daptomycin at low pH range were described by equation

22. In order to obtain the binding parameters the model equation was fit by nonlinear regression to the binding isotherm by WinNonlin. Model predicted curves were shown to describe the experiment data of the titration at pH range of 3.5 to 5 (Table 10 and Figure 51, Appendix C). This suggested that the binding interaction at the pH ranges of 3.5 to 5 were consistent with one site binding model.

Two site model equations (equation 32) were used to describe the data obtained at pH 6 and 7. The binding parameters were estimated by fitting the model equation to the binding isotherm data using nonlinear regression analysis in WinNonlin. The model-predicted isotherms agreed well with experiment data (Figure 52, Appendix C) as shown Figure 27. Furthermore, the residual plots did not show region of systematic bias. The molar signal coefficient (ΔE), the dissociation constant (K_d) and the capacity constant (n) belong to two different types of binding interaction were successfully estimated at each pH value (Table 10).

Table 10 Table show the molar signal coefficient (ΔE), dissociation constant (K_d; μM^{-1}) and capacity constant (n; molecule of daptomycin per one molecule of dendrimer) at first site and second site obtained from individually estimated of the titration at various pH ranges of the binding interaction between daptomycin and PAMAM dendrimer generation 6 (replication = 3)

	Binding parameters											
	First binding site						Second binding site					
	ΔE		K (μM^{-1})		n		ΔE		K (μM^{-1})		n	
pH	Average	SD	Average	SD	Average	SD	Average	SD	Average	SD	Average	SD
3.5	267.43	44.36	0.25	0.03	40.98	8.01						
4	238.33	8.65	0.12	0.04	66.66	3.57						
4.5	265.81	50.20	0.10	0.06	53.00	3.71						
5	207.30	11.38	0.04	0.04	64.81	4.27						
6	269.24	12.93	0.01	0.00	22.96	7.93	-49.97	0.03	1.09	0.40	83.85	5.78
7	258.37	23.94	0.01	0.00	18.01	2.30	-49.97	0.01	2.34	0.79	92.35	3.25

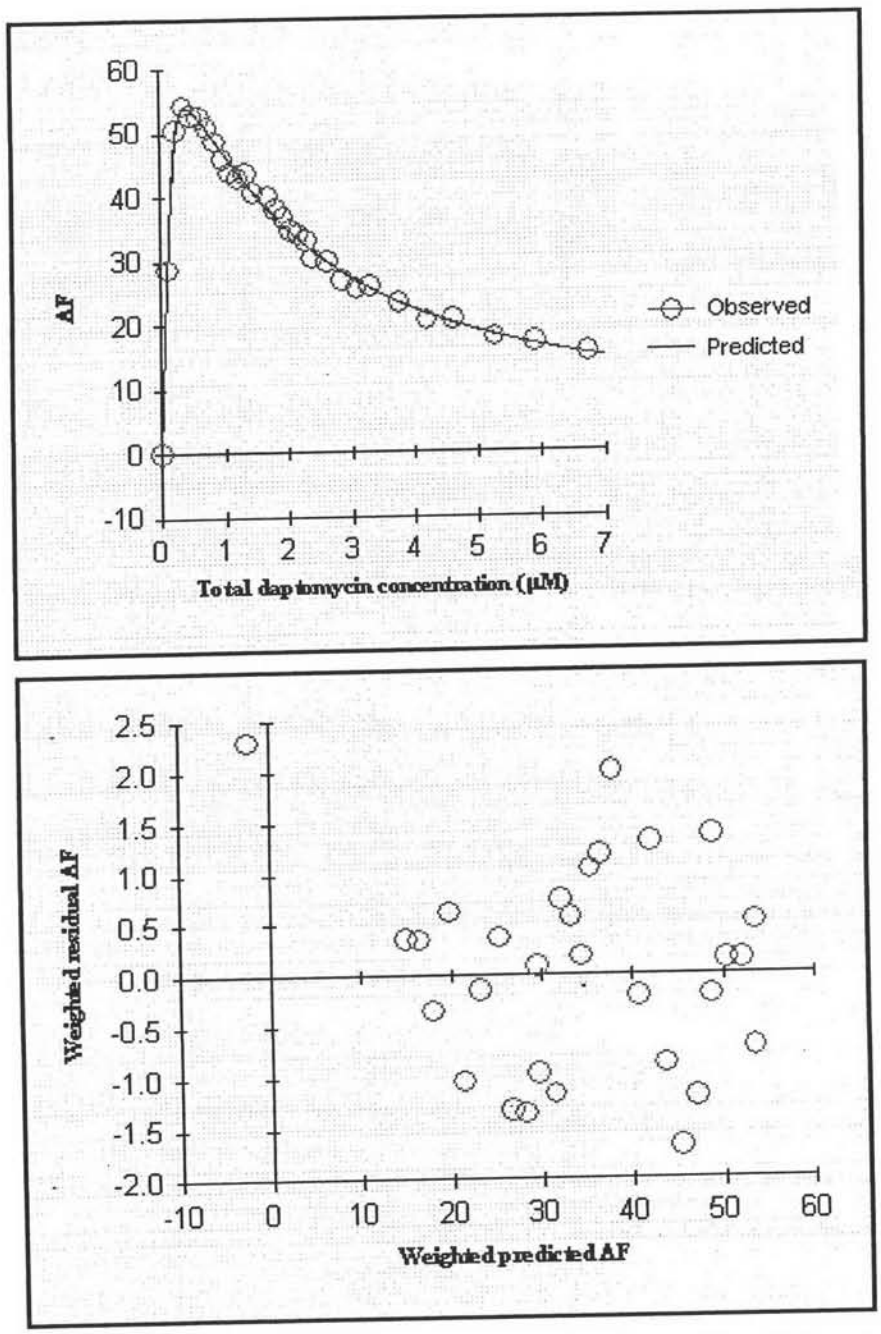

Figure 27 (a) Binding isotherm obtained from the interaction between PAMAM generation 6 and daptomycin at pH 7 and 25°C (opened circle) and fitting curve (solid line), and (b) residuals plot of weighted residual ΔF against weighted predicted ΔF

The values for ΔE_1 and ΔE_2 were essentially constant over the pH range studied (p-value of ΔE_1 and = 0.159 and p-value of ΔE_2 = 0.768) (Table 20, Appendix B), therefore these values were fixed in Equation 32 (ΔE_1 at 251.08 and ΔE_2 at -49.97) and the values for affinity and capacity constants were re-estimated at each

condition by nonlinear regression thereby assigning any remaining variability to the binding properties. All of the predicted curves based on model equations and estimated parameters agreed with the experiment data (Figure 53 to 54, Appendix C). The estimated binding parameters were reported in Table 11. Comparison of the K_{d1} values by one-way ANOVA indicated that these constants were discernibly pH-dependent (Table 21a, Appendix B) and that they could be separated into three groups, estimates associated with pH conditions 3.5, 4-5 and 6-7 (Table 22, Appendix B). The dissociation constant at the second type of binding interaction (K_{d2}) were not discernibly pH-dependent (Table 21b, Appendix B).

Table 11 Dissociation constant (K_d; μM^{-1}) and capacity constant (n; molecules of daptomycin per one molecule of PAMAM dendrimer) at first site and second site obtain from individually estimated of the titration at various pH ranges of the binding interaction between daptomycin and PAMAM dendrimer generation 6 with fixing ΔE_1 and ΔE_2 values at 251.08 and -49.97, respectively. (replications = 3)

	Binding parameters								
	First binding site				Second binding site				
	K_d (μM^{-1})		n		K_d (μM^{-1})		N		
pH	Average	SD	Average	SD	Average	SD	Average	SD	Model
3.5	0.23	0.06	44.41	1.18					1-site
4	0.12	0.04	66.32	5.33					1-site
4.5	0.07	0.02	57.55	6.48					1-site
5	0.08	0.04	57.00	2.61					1-site
6	0.01	0.00	30.69	7.30	1.29	0.70	89.08	6.82	2-site
7	0.01	0.00	19.00	1.17	2.31	0.80	101.02	5.76	2-site

A one-site binding model (equation 22) was used to estimate binding parameters using data generated from the interaction of PAMAM generation 3 and daptomycin at pH 4, whereas, the binding isotherm at pH 7 corresponded to a two site binding model (equation 32). The model equations used at each pH condition fit the experimental data without systematic residual bias and reasonably high correlation coefficients (Figure 55, Appendix C). The estimated binding parameters are displayed in Table 12.

Table 12 The molar signal coefficient (ΔE), dissociation constant (K_d; μM^{-1}) and capacity constant (n; molecules of daptomycin per one molecule of PAMAM dendrimer) at first site and second site obtain from individually estimated of the titration at various pH ranges of the binding interaction between daptomycin and PAMAM dendrimer generation 3 (replications = 3)

	Binding parameters											
	First binding site						Second binding site					
	ΔE		K (μM^{-1})		n		ΔE		K (μM^{-1})		n	
pH	Average	SD	Average	SD	Average	SD	Average	SD	Average	SD	Average	SD
4	215.60	12.85	0.56	0.03	13.94	1.12						
7	204.94	20.90	0.01	0.00	5.85	0.19	-41.20	7.71	0.50	0.07	15.13	2.84

All data set were simultaneously fitted to the nonlinear equation 22 and 32. All replicated data sets with the same condition were fitted with the same model. The resultant model predicted curves agreed with the experiment data and the resulting in the binding parameters estimates are given in Table 13 (Figure 56 to 59, Appendix C). All binding isotherms were re-fit using fixed values for ΔE_1 and ΔE_2 based on the average value of 240.13 and -46.65. The estimated binding parameters are reported in Table 14. These estimates are not different from those obtained initially by treating each data set separately (Figure 60 to 63, Appendix C).

Table 13 The molar signal coefficient (ΔE), dissociation constant (K_d; μM^{-1}) and capacity constant (n; molecules of daptomycin per one molecule of PAMAM dendrimer) at first site and second site obtained from simultaneous estimated of the binding isotherm at various pH ranges of the binding interaction between daptomycin and various PAMAM dendrimer generation

		Binding parameters					
		First binding site			Second binding site		
Generation	pH	ΔE	K_d	n	ΔE	K_d	n
3	4	208.44	0.59	14.11			
	7	202.23	0.01	5.85	-39.74	0.54	12.5
5	3.5	257.90	0.41	47.01			
	4	244.27	0.07	57.88			
	4.5	261.03	0.11	54.30			
	5	207.39	0.02	13.33			
	6	205.52	0.03	11.23			
	7	219.43	0.06	8.99			
	8	215.21	0.03	7.50			
6	3.5	287.02	0.27	37.54			
	4	239.46	0.12	66.19			
	4.5	265.68	0.10	52.42			
	5	205.96	0.04	64.81			
	6	255.76	0.01	32.84	-47.43	1.74	86.30
	7	257.12	0.01	17.82	-49.02	2.32	93.51

Table 14 Dissociation constant (K_d; μM^{-1}) and capacity constant (n; molecules of daptomycin per one molecule of PAMAM dendrimer) at various pH ranges of the binding interaction between daptomycin and various PAMAM dendrimer generation estimated by simultaneous fitting using WinNonlin software with fixing the molar signal coefficient (ΔE_1 and ΔE_2) as a constant at 240.13 and -46.65, respectively

		Binding parameters			
		First binding site		Second binding site	
Generation	pH	K_d	n	K_d	n
3	4	0.76	12.71		
	7	0.01	5.52	0.26	12.72
5	3.5	0.33	49.45		
	4	0.06	58.55		
	4.5	0.05	57.54		
	5	0.13	12.07		
	6	0.13	9.95		
	7	0.11	8.37		
	8	0.06	6.78		
6	3.5	0.22	44.27		
	4	0.12	65.98		
	4.5	0.07	57.30		
	5	0.07	56.63		
	6	0.01	34.63	1.73	81.94
	7	0.01	19.17	2.00	90.85

4.2.2. Evaluation of the relationship between ionic form of the reactants and binding constants

The estimated capacity constants for the interaction of daptomycin and PAMAM generation 6 were not discernibly pH-dependent. This observation is consistent with the results obtained using PAMAM generation 5. However the binding capacities were pH-dependent for all PAMAM substrates. The relationship between the ionic state of the reactants and PAMAM generation 6 dendrimers is displayed in Figures Figure 28 and 29.

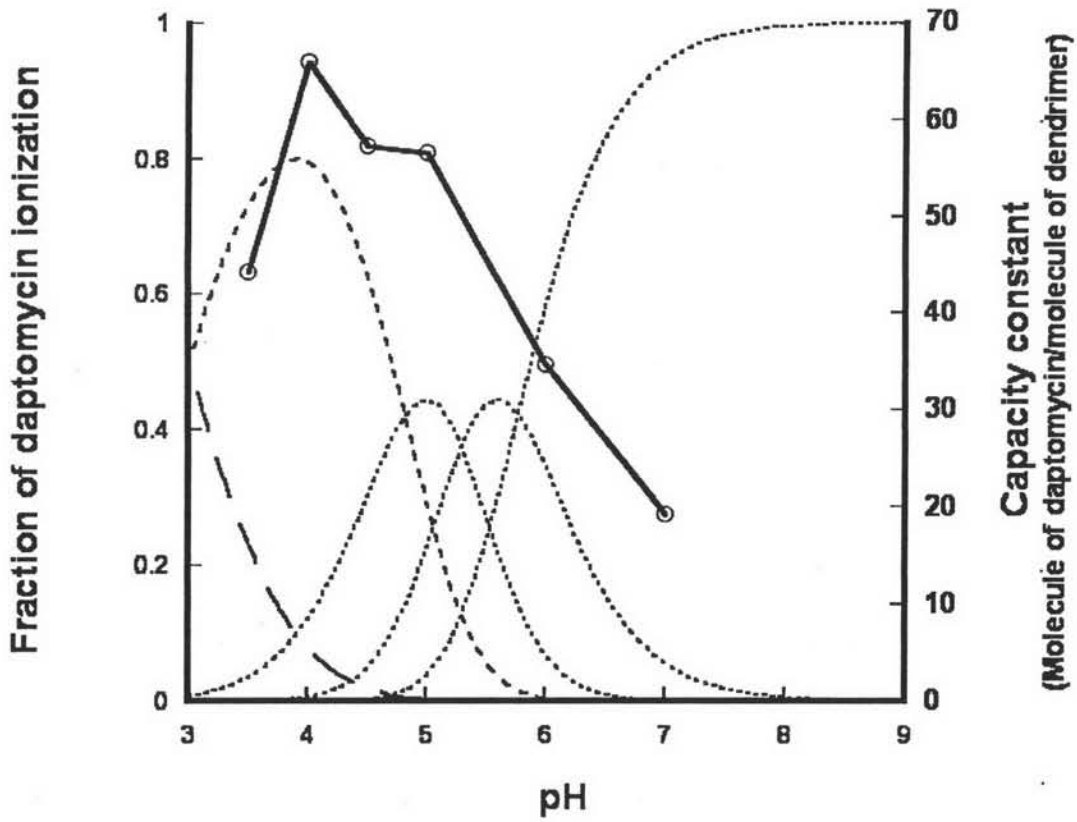

Figure 28 Comparison between the distribution of ionic forms of daptomycin and the estimated binding capacities for its interaction with PAMAM generation 6. Fraction of daptomycin ionization varied from (— —) cation, (- - -) zwitterion, (·····) anion, dianion and trianion, respectively. Each point (-⊖-) represented the capacity constant at various pH.

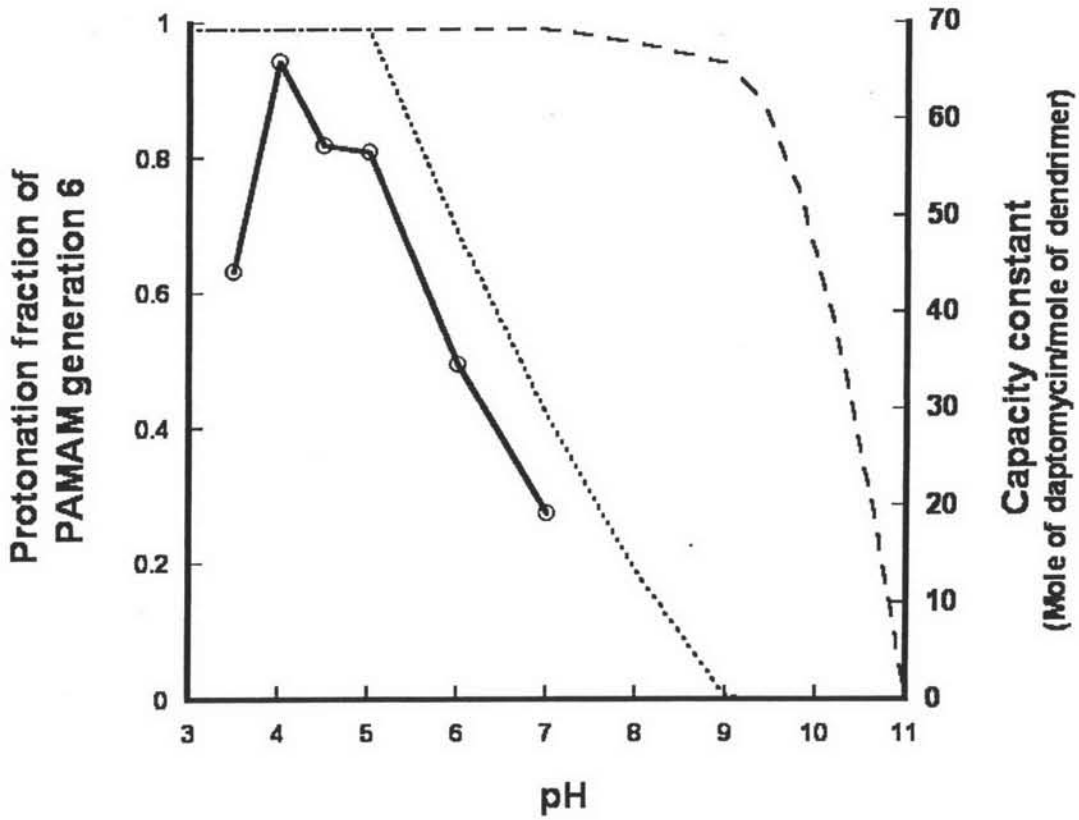

Figure 29 Comparison of ionization of PAMAM generation 6 to the estimated binding capacity for its interaction with daptomycin. The tertiary amines (·····) gradually deprotonate from pH 5 to pH 9, whereas primary amines (- - -) deprotonate after pH 7. Each point (-O-) represented the capacity constant at various pH.

Two observations can be made based on the comparisons displayed in Figures 28 and 29. Firstly, the major determinant in the magnitude of the binding capacity appears to be the presence of the zwitterionic form of daptomycin (Figure 28). This observation is consistent with the relationship observed for PAMAM generation 5 (Figure 23).

Secondly, the decrease in the estimated capacity constant observed in the pH range 5 to 7 appears to correlate to the deprotonation of the dendrimer tertiary amines (Figure 29). This observation is more distinct for capacity constants estimated for PAMAM generation 6 interactions (Figure 29) than with PAMAM generation 5 (Figure

24), i.e. the capacity constant change in this pH range in Figure 24 (generation 5) is more subtle than in Figure 29 (generation 6). This result could be explained based on the gradual loss on interior electrostatic repulsion over this pH range resulting in increasingly condensed dendrimer structures (Maiti et al., 2005) and reduced surface areas for daptomycin interaction. This explanation is consistent with the larger pH-dependent capacity constant change observed for the larger dendrimer (generation 6) over the range of pH values associated with tertiary amine deprotonation.

The two site model for G6 dendrimers appeared to be relevant only at neutral pH values wherein the interactions between dendrimers were not optimal based on dendrimer surface area and the daptomycin molecules were highly anionic. This result suggests that in the presence of relatively high concentrations of tri- and di-anionic daptomycin species some deterioration of surface binding occurs perhaps due to "sharing" of daptomycin charge over several dendrimer molecules as has been previously suggested (Section 3.1.1).

4.2.3. Evaluation of the effects of pH and dendrimer size using multivariate linear regression

A linear model containing two factors (PAMAM generation size and pH of the system) was used to evaluate their effects on capacity constant estimates. PAMAM generation size consisted of 3 levels which are generation 3, 6 and 5. The pH of the system had 2 levels which are pH value of 4 and 7. Visualization of confidence intervals was applied to F-test by using a leverage plot (Figure 30). The response was capacity constant whereas the two factors were PAMAM generation size and pH. The results of the analysis are displayed in four panels illustrating the overall model results, main effects, and interaction effects. In Figure 30, the overall mean response is displayed as a horizontal line; the actual values of capacity constant are plotted as a function of each effect; the predicted values of capacity constant are plotted versus the effect level as a regression line with 95% Confidence Intervals (CI) on the model predicted values. The significance of each effect was indicated by the comparison of the CI and the overall mean response. When the CI crosses the overall mean response line, it signifies a significant effect. In this study, both PAMAM generation size and pH appeared to be a significant main effect while interaction effects of generation size and pH were not significant.

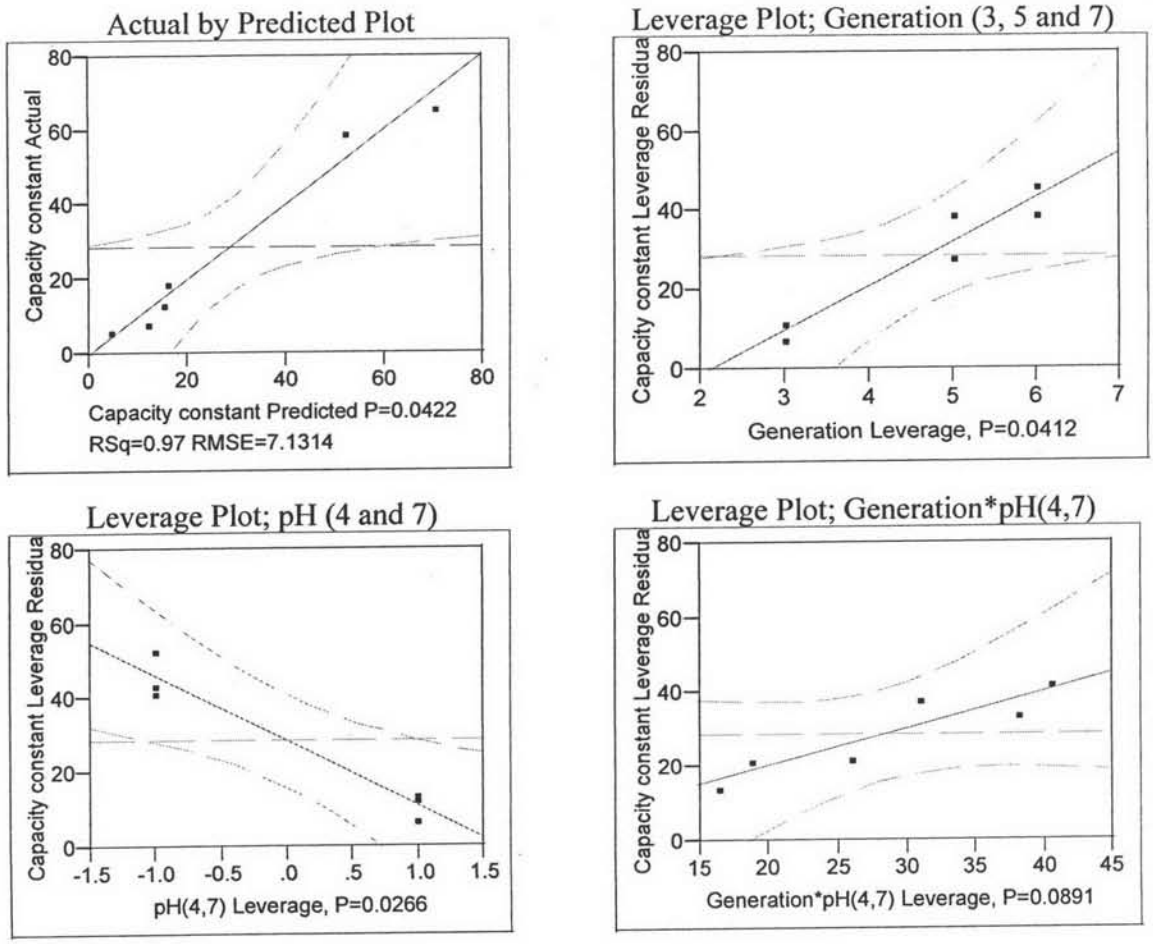

Figure 30 Actual and leverage plot of multivariate linear model using JMP 5.0.1 software. The model contained two factors which are PAMAM generation size and pH of the system. PAMAM generation size consisted of 3 levels which are generation 3, 6 and 5. The pH of the system had 2 levels which are pH value of 4 and 7.

4.3. Development of molecular model for the interaction between daptomycin and PAMAM dendrimer

The ability of daptomycin to associate to PAMAM dendrimer has been demonstrated by fluorescence spectroscopy. The nature of the interaction as indicated by the shape of the binding isotherm and the dependence of the estimated capacity constants on dendrimer size and solvent pH provide meaningful insight into the mechanisms of interactions. A number of deductions have been described herein and are summarized below:

4.3.1. Interactions between daptomycin and dendrimers are accompanied by fluorescence changes (enhanced tryptophan quenching and kynurenine emission with some blue-shifting) that are consistent with a decrease in the conformational flexibility in the microenvironments associated the fluorophores (kynurenine and tryptophan).

4.3.2. A one site binding model adequately describes the binding isotherm obtained under a variety of experimental conditions and with dendrimers of various sizes except under pH conditions where binding is marginal or non-existent (i.e. pH < 3 and pH ≥ 7).

4.3.3. For all of the dendrimers studied. optimal binding occurs in the pH region 3.5 to 4.5 wherein both the external and internal dendrimer amines are protonated and daptomycin is in its zwitterionic form. Since the most likely scenario for the intermolecular interactions is based on electrostatic attraction, the optimal conditions appear to be those wherein the deprotonated asp-3 of daptomycin (pKa ≈ 3) interacts with surface amines on the dendrimer and causes no net change in dendrimer surface charge. The orientation of the daptomycin molecules and their position within or on the surface of the dendrimer can be rationalized based on considerations of molecular conformations and size. These considerations are developed below.

4.3.4. Another important observation is the decrease in binding capacity that occurs in the pH region 5 to 7. The observed capacity constant change was greater for data obtained using the larger dendrimer (generation 6) than for that obtained using a smaller macromolecule (generation 5). In this pH region, the daptomycin molecule is progressively more anionic in moving from lower to higher pH values, and therefore one might anticipate that the electrostatic interactions would become stronger. In fact, the affinity constant does not change appreciably but the capacity constants decrease rather

than increase. The lack of a significant affinity constant change is consistent with the primary electrostatic interaction occurring between asp-3 of daptomycin and dendrimer surface amines because the ionicity of neither of these species changes in this pH region. The decrease in capacity constant can be rationalized by a progressive condensation of dendrimer size due to the deprotonation of interior amines and the loss of internal electrostatic repulsion. This explanation also accounts for the larger capacity decrease observed for the larger dendrimer wherein the surface area change would be predicted to be greater.

An attempt to further develop the spatial and orientation relationships involved in daptomycin-PAMAM dendrimer interactions was undertaken by examining the published conformations of these two molecules and predicting the maximum capacity constants based on molecular orientation and size.

The conformation of free daptomycin was downloaded from RCSB protein data bank. This conformation was proposed by Jung et al. using Nuclear Overhauser Enhancement Spectroscopy (NOESY) techniques (Jung et al., 2004). A space filling or CPK model of daptomycin was regenerated using Chem3D Ultra 10.0. The model showed atoms as three-dimensional spheres whose radii are scaled to the atoms' van der Waals radii.

There were two possible orientational extremes to be considered for daptomycin: one in a longitudinal orientation (Figure 31) and the other in a latitudinal orientation (Figure 32). The longitudinal and latitudinal orientations were estimated to be 24.5 and 14.9 Å, respectively.

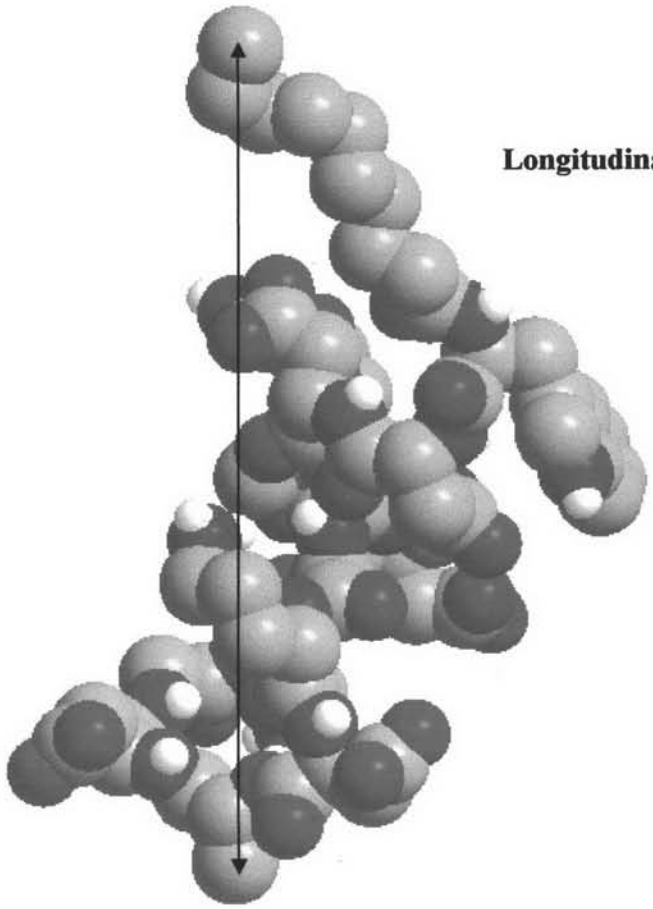

Figure 31 Space filling model showing the measurement of daptomycin diameter in longitudinal dimension using Chem3D

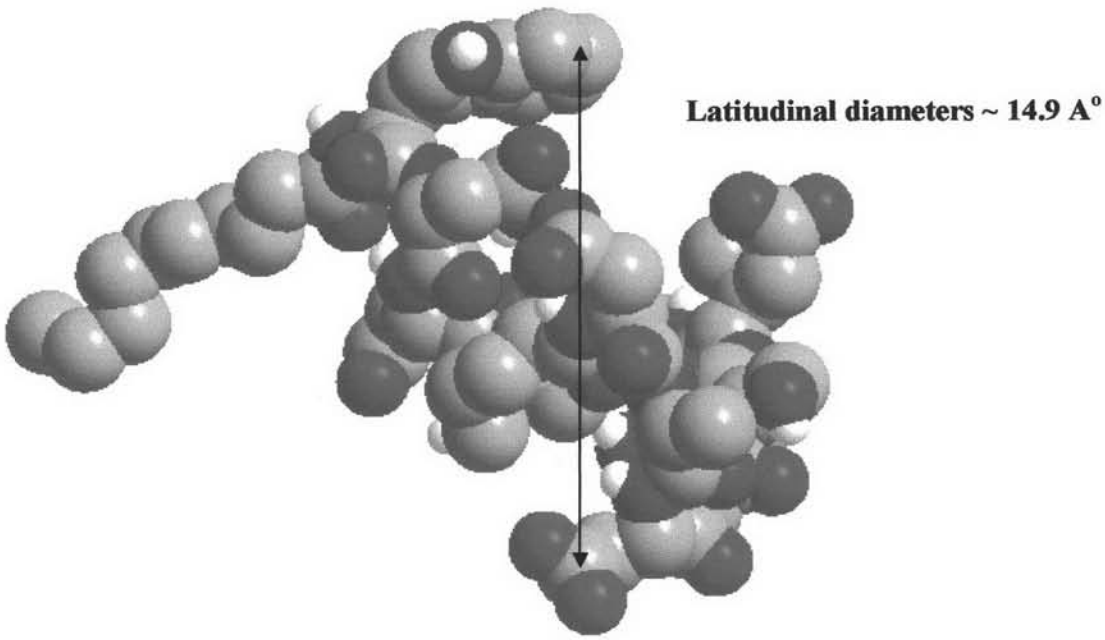

Figure 32 Space filling model showing the measurement of daptomycin diameter in latitudinal dimension using Chem3D

As described in equation 14, the maximum theoretical binding capacity for ligand bound to dendrimer surface is give by the ratio of the dendrimer surface areas to the cross sectional area of the ligand. Assuming a spherical PAMAM dendrimer and published PAMAM dendrimer diameters (Jackson et al., 1998), the estimated dendrimer surface areas are displayed in Table 15.

The cross sectional area for daptomycin depends on its orientation. Based on the two orientational extremes described above, circular cross-sectional areas were estimated (Table 15).

Table 15 Table showed the calculated cross sectional areas of daptomycin and surface area of dendrimer

	Daptomycin		Dendrimer		
	Longitudinal	Latitudinal	3rd	5th	6th
Area (Å)	471.74	174.44	3020.29	8828.29	14108.29

The maximum theoretical binding capacities of various dendrimers for daptomycin molecules oriented latitudinally or longitudinally (Figure 33) were predicted and are compared to the experimentally measured maximum capacity constants (Table 16). For all of the dendrimers, the predicted theoretical capacities using a latitudinal orientation are in reasonable agreement with the observed values suggesting that daptomycin is capable of nearly completely covering the dendrimer surface under pH conditions wherein binding is optimal (pH 3.5 to 4.5).

Table 16 Table showed the calculated theoretical capacity and observed capacity obtained from fluorescence titration technique

Generation	Theoretical capacity		Observed capacity
	Latitudinal	Longitudinal	
3	17	6	13
5	51	19	59
6	81	30	67

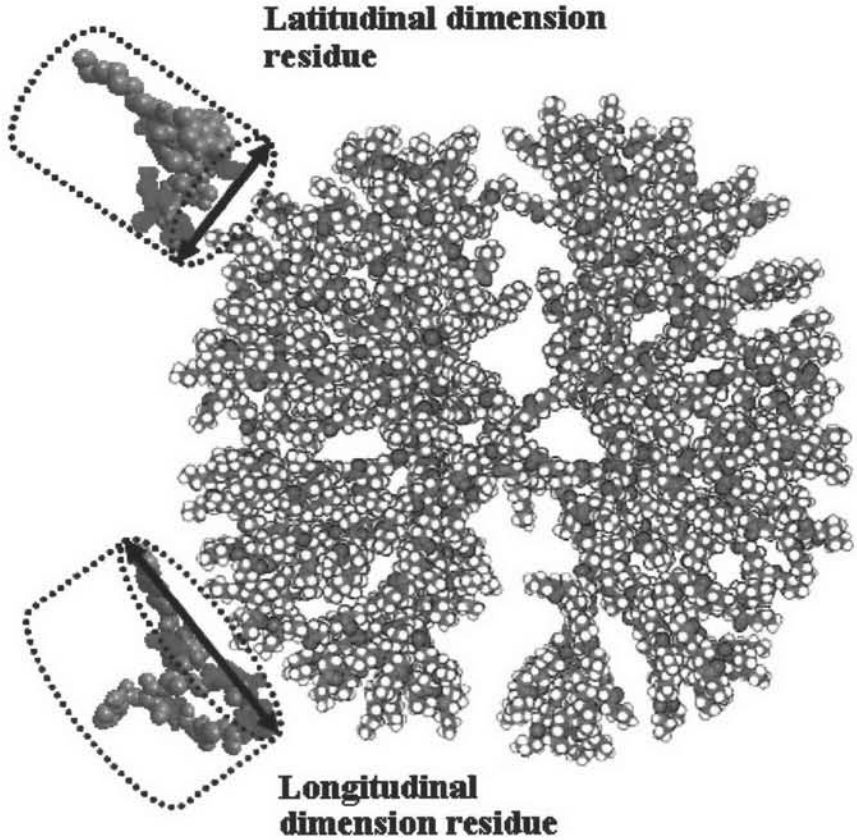

Figure 33 Possible conformation of daptomycin in bound state including latitudinal dimension residue and longitudinal dimension residue

The latitudinal orientation can occur in two ways. Either the cyclic peptide portion of daptomycin is on the surface of the dendrimer or the lipoidal tail is insert into the dendrimer is such a way that effective electrostatic interactions can occur. The later option seems more likely based on two considerations. Firstly asp-3 is situated near the lipid tail whereas the cationic ornthine residue is present in the cyclic peptide portion of daptomycin. The protonated ornithine side chain would be expected to repel and not attract the protonated surface amines of the dendrimer whereas the anionic side chain carboxylate of asp-3 should be an effective counterion for the cationic dendrimer surface.

Secondly the effect of binding on daptomcyin fluorophores favors an interaction involving lipid tail insertion. Upon binding, both of tryptophan and kynurenine emission maxima were shifted approximately 5 nm toward the shorter

wavelengths (blue shifted) (Figure 34). This type of blue shift for tryptophan emission maxima has typically been attributed to its presence in conformationally-restricted or hydrophobic environments (Chen, Ludescher and Montville, 1998; Yu et al., 2001; Lakowicz, 2007). In addition, the blue shifted in fluorescence emission of daptomycin was also observed in the membrane interaction at a presence of calcium (Lakey and Ptak, 1988). Therefore, the observed blue shift likely indicates that the tryptophan residue on the daptomycin molecule conformationally-restricted and hydrophobic region. Thus the likely involvement of asp-3 and flurophore changes associated with tryptophan and kynurenine all suggest a latitudinal orientation with lipid tail insertion into the dendrimer as illustrated in Figure 35.

The observed decrease in capacity constants in the pH region 5 to 7 is consistent with this model based on the expected decrease in dendrimer surface area due to internal structural condensation. But a reasonable alternative explanation is that increased electrostatic repulsion of daptomycin molecules due to increased ionization of the carboxylate residues prevents their tight packing on the dendrimer surface.

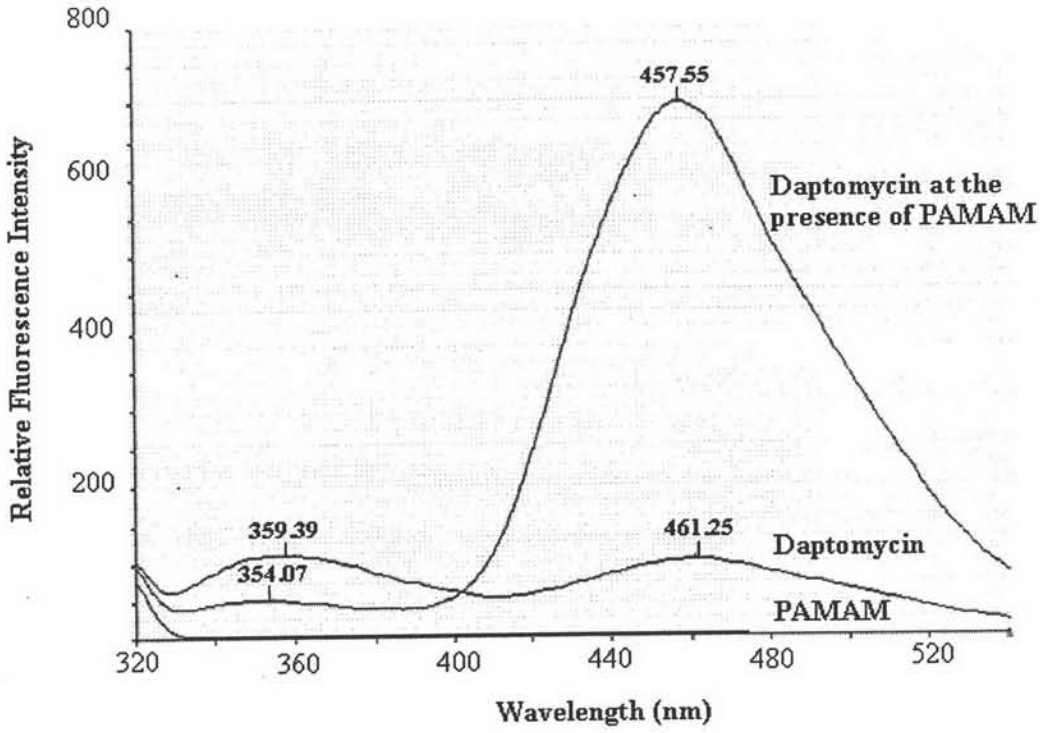

Figure 34 Fluorescence emission spectra of the PAMAM generation 5 solution, daptomycin and mixtures of daptomycin and PAMAM generation 5

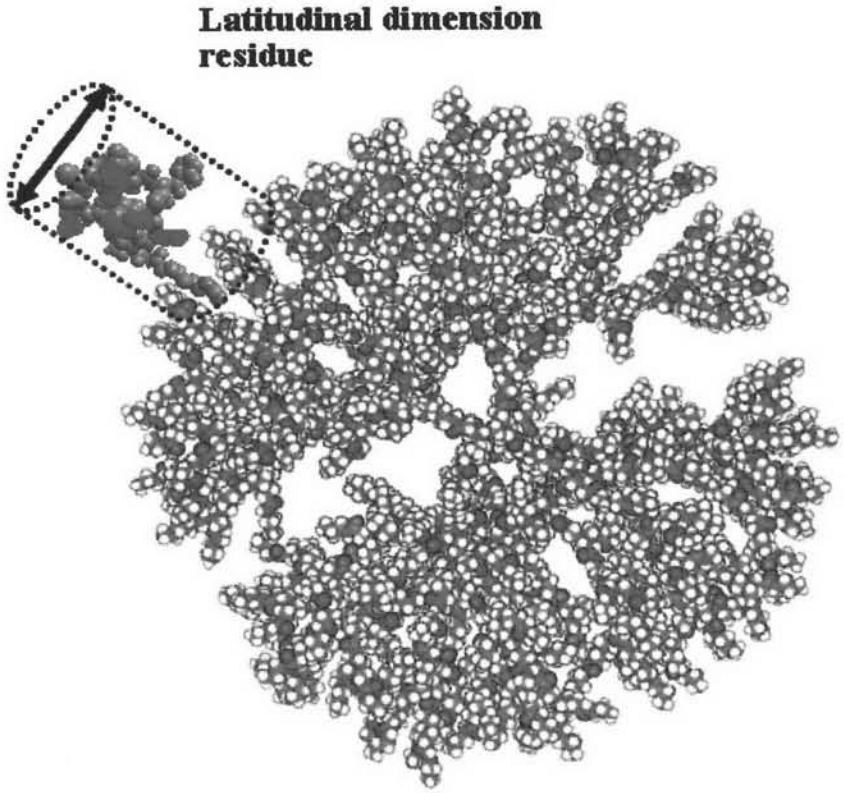

Figure 35 Proposed daptomycin in bound state in latitudinal dimension residue with decanoyl chain insertion

4.4. Relationships between binding models, parameter values and binding isotherm shapes

The use of binding isotherm shape to identify an appropriate binding model was investigated by predicting a series of binding isotherms using the equations associated with various binding model equations and wherein the binding parameters were varied in such a way as to discern their effects on binding shape. Then typical experimentally observed binding isotherms were compared to the series of model predicted profiles in order to determine whether inferences could be reasonably made.

4.4.1. Model-predicted one site binding isotherm

Data sets were simulated using Equation 22 (Excel, Microsoft). The three parameters including molar signal coefficient (ΔE), dissociation constant (K_d) and the total number of independent binding sites (R) were individually varied to illustrate the effect of the binding parameters on the isotherm profiles and to provide reasonable ranges for each parameter for the determination of the upper and lower initial parameters in the curve fitting procedure.

The ΔE was varied from 100 to 300, while both K_d and R were fixed at·0.01 μM^{-1} and 232.11, respectively. As shown in Figure 36, increasing in ΔE resulted in increases of both plateau level and slope of the initial phase of the binding isotherm. However, the change in slope of the initial phase of the binding isotherm was not observed in typical binding isotherms obtained from titration of PAMAM generation 5 with daptomycin at pH range of 3.5 to 8 and the titration of PAMAM generation 6 with dendrimer at pH range of 3.5 to 5 (Figure 21 and Figure 25). In addition, the estimated ΔE values obtained from those isotherms were not determined to be statistically different (Table 18 and 20a, Appendix B). Taken together these observations confirm that the ΔE value was essentially constant. In addition, model predicted curve with ΔE equal to 232.11 to the observed data set from titration of PAMAM generation 5 at pH 5 (circle) suggested initial values for curve fitting.

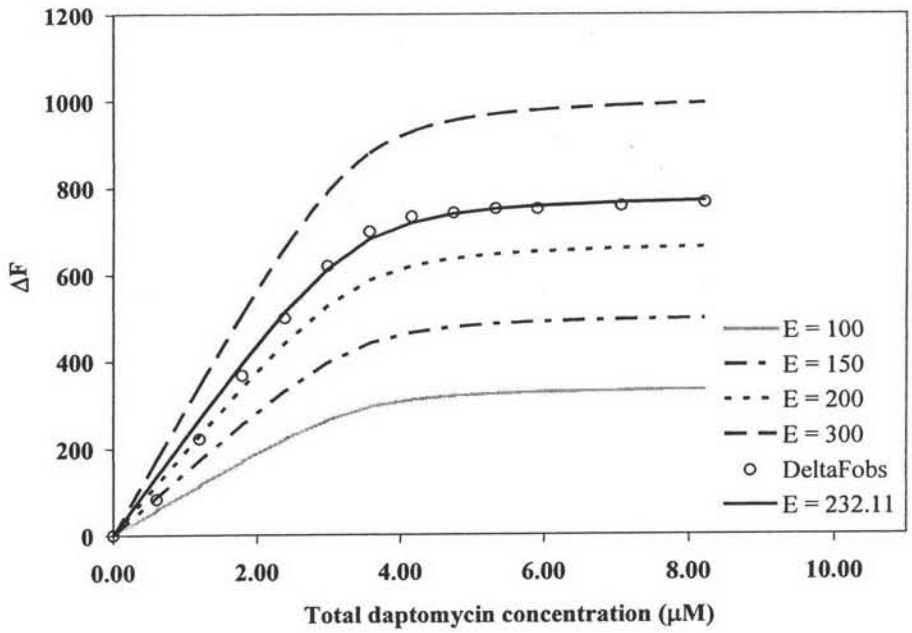

Figure 36 Simulation plots showing the effect of molar signal coefficients or ΔE on the profile changes in the one type binding isotherm

Another series of simulated binding isotherms were generated using to one site model equation with various K_d values ranging from 0.001 to 2 and fixed values of R and ΔE at 3.5 and 232.11, respectively (Figure 37). The simulated profiles suggest that increasing the K_d values suppresses the slope and curvature. Higher K_d values indicate less affinity between ligand and substrate. The change in the slope and curvature were not observed in the experimentally obtained isotherms using PAMAM generation 5 at pH 4 to 8 and statistical evaluation did not indicate significant differences between the estimated K_d values (Table 19, Appendix B). Taken together, these observations suggest that the K_d was essentially constant of the conditions studied and that reasonable initial values of K_d for curve-fitting procedures was 0.1 μM^{-1}.

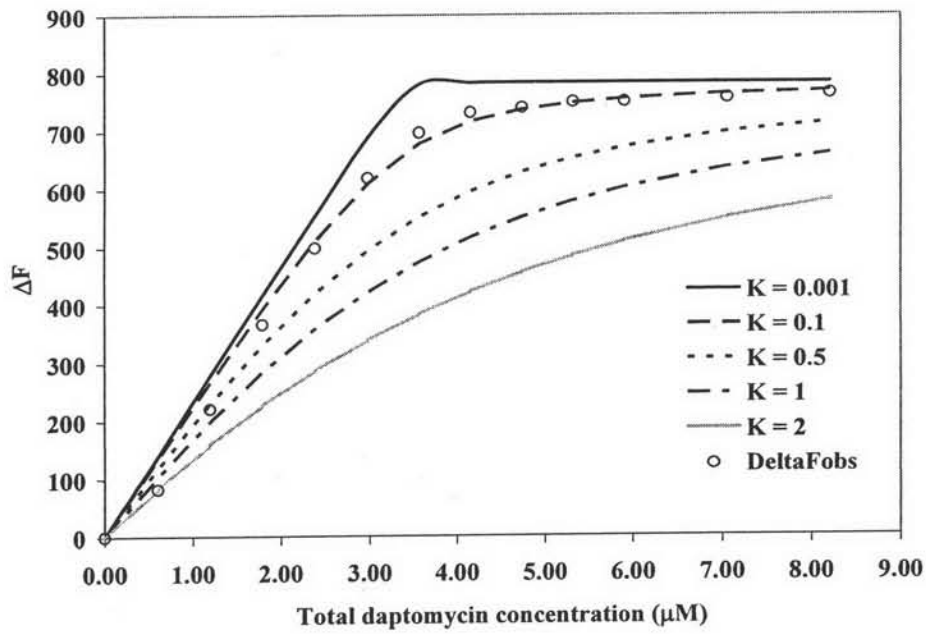

Figure 37 Simulation plots showing the effect of dissociation constants or K_d on the profile changes in the one type binding isotherm

The effect of the capacity constant (R) on the shape of the isotherm was evaluated by conducting simulations using R values from 1.5 to 5.5 wherein both of K_d and ΔE fixed were fixed at 0.1 μM^{-1} and 232.11, respectively. Increasing R value appeared to increase the isotherm plateau without changing the slope (Figure 38). This behavior is very similar to that observed with experimentally obtained isotherms and suggests that the primary source of difference between the experimentally-obtained isotherms (one-site binding model) was, in fact, changes in the capacity constant. For the titration of PAMAM generation 5 and daptomycin at pH 5, the initial value of R appeared to be 3.5.

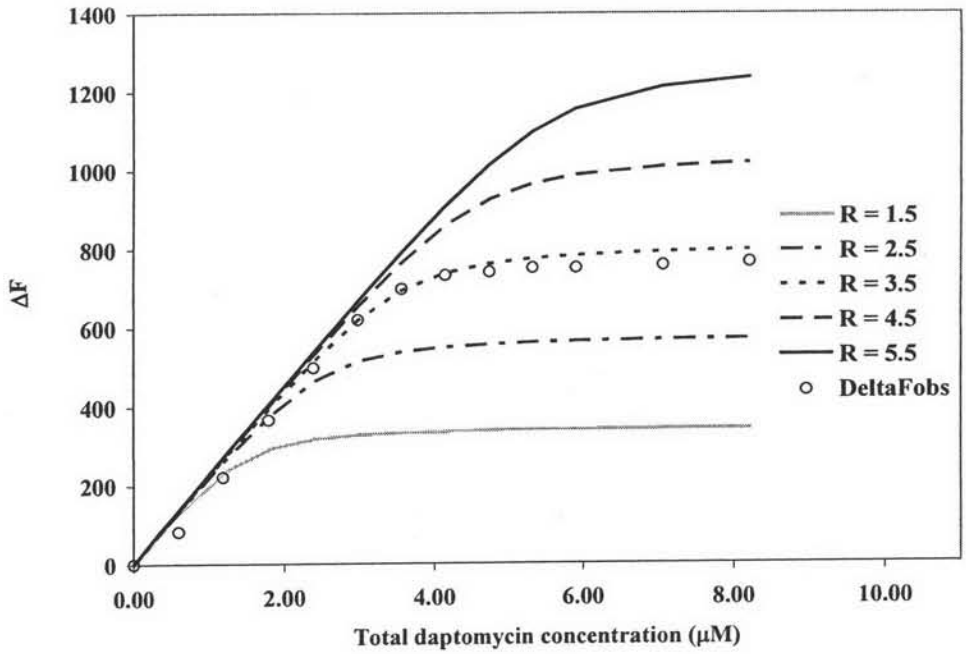

Figure 38 Simulation plots showing the effect of total number of independent binding sites or R on the profile changes in the one type binding isotherm

4.4.2 Model-predicted two site binding isotherm

Simulations using two site binding site model equations resulted in biphasic isotherms involving six parameters including two molar signal coefficients (ΔE_1 and ΔE_2), two dissociation constants (K_{d1} and K_{d2})and two capacity constants (R_1 and R_2).

Simulations using equation 32 and varying ΔE_1 value from 100 to 500 while fixing the rest of the parameters to be -40, 0.01, 1, 0.31 and 1.2 for ΔE_2, K_{d1}, K_{d2}, R_1 and R_2, respectively, are depicted in Figure 39a. A typical experimental data set is also depicted using the results from the titration of PAMAM dendrimer generation 6 with daptomycin at pH 7. Simulations were also generated by varying ΔE_2 from -100 to 40 wherein the rest of the parameters were fixed as described above and the ΔE_1 value was fixed at 300 (Figure 39b). The effect of varying ΔE_1 values was similar to that previously observed in the one site binding model simulations involving variable ΔE values. Increase in ΔE_1 value brought about a decrease in both maximum ΔF and the slope of the curve. Comparisons of the simulations generated by varying ΔE_1 values with those obtained by varying ΔE_2 values revealed some differences. ΔE_1 values exerted their

influenced throughout the profile, whereas ΔE_2 values only played a role in the depletion phase or the second phase of the binding isotherm. Giving positive and zero value of ΔE_2 showed no difference in binding profile from the one site binding isotherm, whereas the binding profiles with negative ΔE_2 values exhibited biphasic behavior. Therefore, a negative value for ΔE_2 was consistent with experimental observations for daptomycin-dendrimer interactions at pH 7. The lack of an ascending slope change and the absence of increasing concavity at different pH values suggests that the values of both ΔE_1 and ΔE_2 did not change with changing experimental conditions. In addition, the reasonable initial value of ΔE_1 and ΔE_2 were determined to be 300 and -40.

a

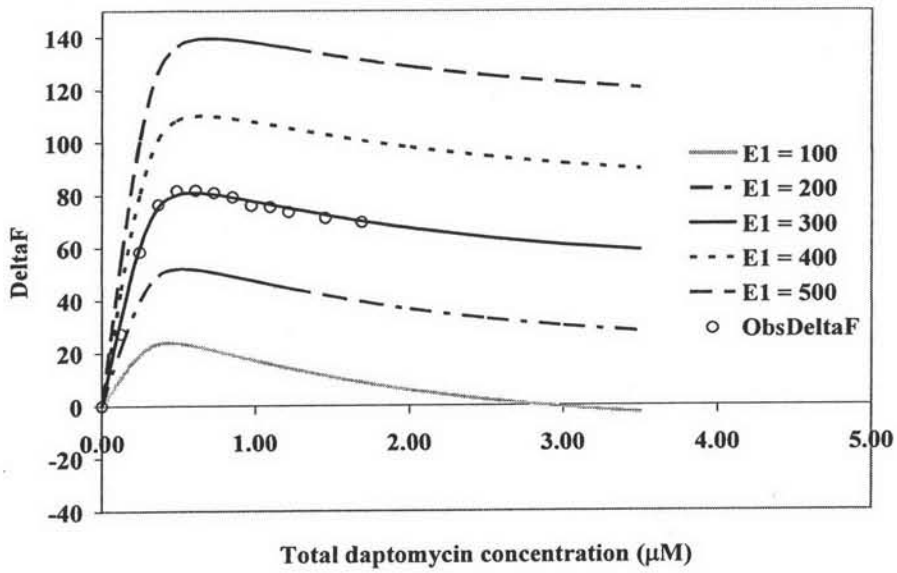

b

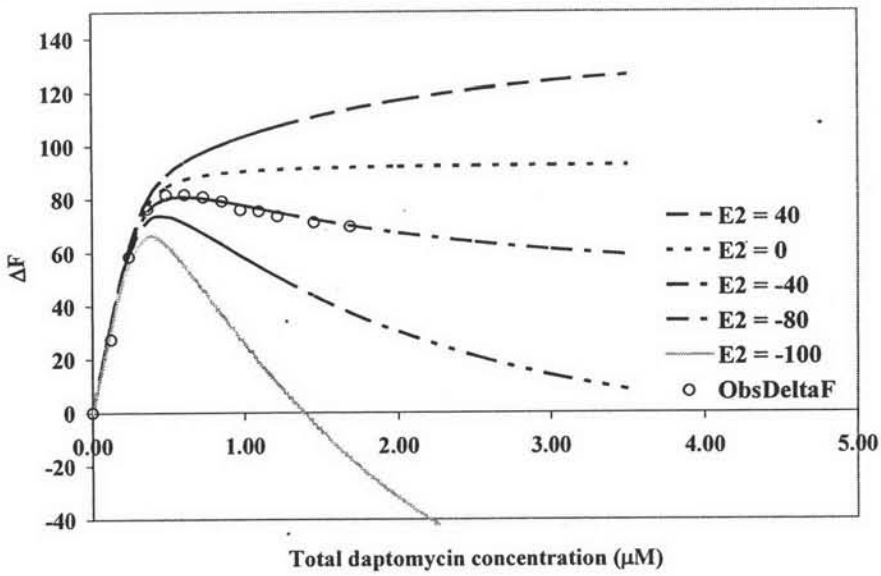

Figure 39 Simulation plots showing the effect of molar signal coefficients or ΔE of first binding type (a) and second binding type (b) on the profile changes in the one type binding isotherm

The effect of varying K_{d1} and K_{d2}.was evaluated in a series of simulations using two site model equations and fixing the remaining parameters at 300, -40, 0.01, 1, 0.31 and 1.2 for ΔE_1, ΔE_2, K_{d1}, K_{d2}, R_1 and R_2, respectively (Figure 40). A typical experimental data set from the titration of PAMAM dendrimer generation 6 with daptomycin at pH 7 is displayed in Figure 40. Comparison of the simulations varying K_{d1} with those varying K_{d2} indicated that both parameters influenced on the slope and the curvature of the profile and their influences were interrelated. A decreasing K_d implies increasing affinity. Increasing K_{d1} value or reducing affinity of first binding type caused decrease in the slope and the curvature concavity. If the first site possesses a low affinity, then influence of the affinity from the second site predominates. Whereas an increase in the binding affinity of second site results in complex behavior strongly related to the K_{d1} value (Figure 40). If the value of K_{d2} was much less than the K_{d1} value, a lag phase was observed (Figure 40b). Reasonable initial values for the dissociation constant were determined to be 0.01 and 1 for K_{d1} and K_{d2}, respectively.

a

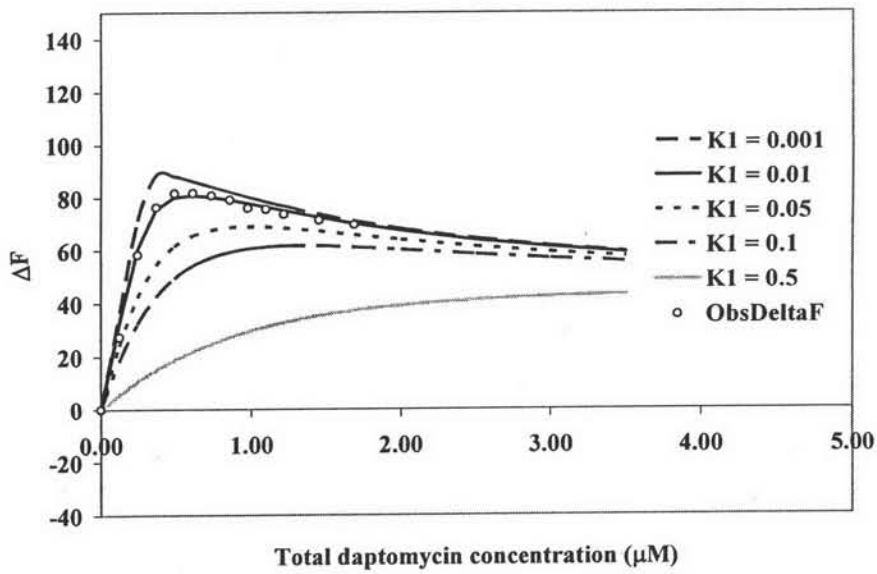

b

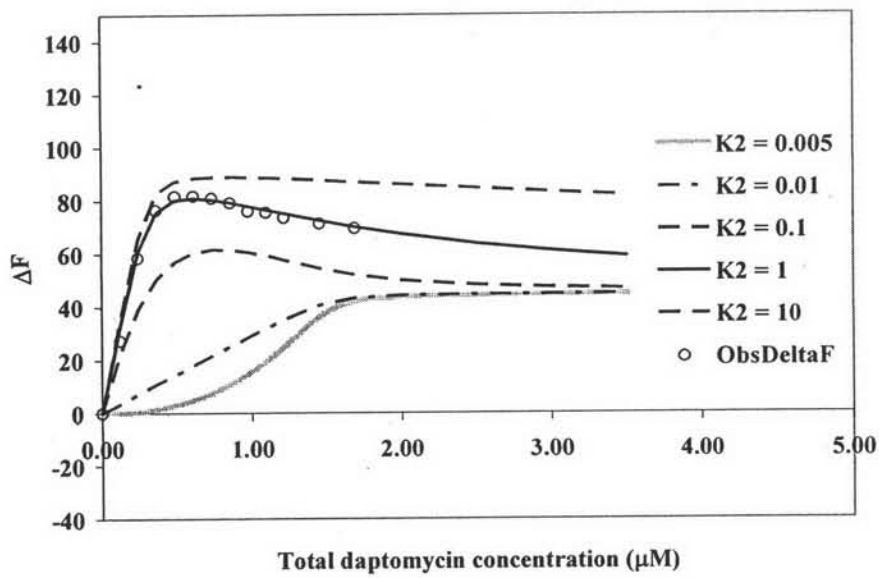

Figure 40 Simulation plots showing the effect of dissociation constant or K_d of first binding type (a) and second binding type (b) on the profile changes in the one type binding isotherm

The effects of R1 and R2 values on isotherm characteristics were individually studied. The rest of the parameters again were fixed. The observed isotherm was obtained from the titration of PAMAM dendrimer generation 6 with daptomycin at pH 7 (Figure 41). The effect of R_1 was similar to the behavior of R in the simulation of one site binding site. Increase in R_1 resulted in an increase in increased maximum fluorescence intensity as shown in the Figure 41a. Whereas increased R_2 values affected the second phase of the binding isotherm as shown in Figure 41b. The increasing R_2 value resulted in the depletion of ΔF. The initial value used for the fitting of binding isotherm obtained from the titration of PAMAM dendrimer generation 6 with daptomycin at pH 7 were selected to be 0.3 and 1.2 for R_1 and R_2, respectively.

a

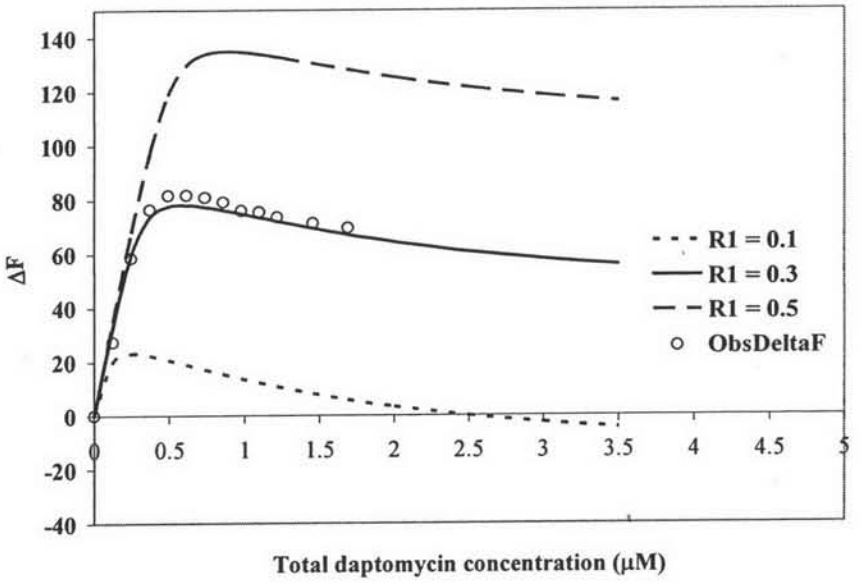

b

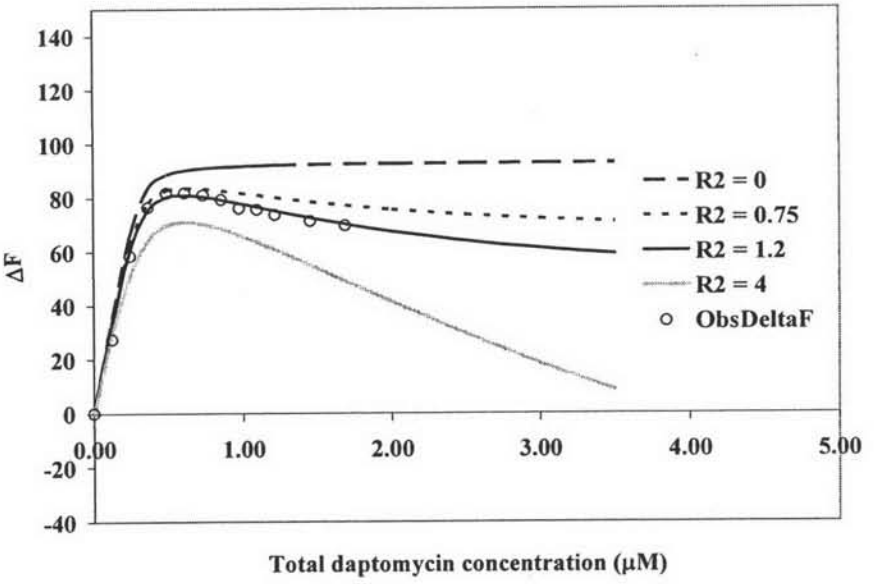

Figure 41 Simulation plots showing the effect of total number of independent binding sites or R of first binding type (a) and second binding type (b) on the profile changes in the one type binding isotherm

5. Prediction of Optimum Total Dendrimer Concentration

From a delivery system design viewpoint the identification of the optimal conditions to load dendrimers with daptomycin is an important consideration. From the moles of daptomycin bound ([Den-Dap]) per mole of total dendrimer ($[Den]_T$);

$$r = \frac{[Den - Dap]}{[Den]_T} = \frac{n \times [Dap]}{K_d + [Dap]} \qquad \text{equation 33}$$

where r represents moles of daptomycin bound ([Den-Dap]) per mole of total dendrimer ($[Den]_T$). [Dap] is free daptomycin concentration. K_d and n represent dissociation constant and independent binding sites, respectively. Equation 33 can be rearrange to

$$[Den - Dap] = [Den]_T \times \left(\frac{n \times [Dap]}{K_d + [Dap]} \right) \qquad \text{equation 34}$$

The fraction of daptomycin bound is defined as following.

$$\text{Fraction of Daptomycin bound} = \frac{[Den - Dap]}{[Dap]_T} \qquad \text{equation 35}$$

Substitution of equation 34 to equation 35 yields

$$\text{Fraction of Daptommycin bound} = \frac{[Den]_T}{[Dap]_T} \times \left(\frac{n \times [Dap]}{K_d + [Dap]} \right) \text{equation 36}$$

Given binding capacity relationship to pH (Table 12), the optimal conditions using PAMAM generation 6 would appear to be pH 4. The K and R values were 0.12 μM^{-1} and 65.98, respectively. The total concentration of daptomycin was fixed at 3 μM. Substitution of the binding parameters and total daptomycin concentration into equation 36 provided following equation.

$$\text{Fraction of Daptommycin bound} = \frac{[Den]_T}{3} \times \left(\frac{65.98 \times [Dap]}{0.12 + [Dap]} \right)$$

The fraction of bound-daptomycin as a function of total daptomycin concentration was estimated based on single site model equations and the parameters obtained from experimental data using PAMAM generation 6 at pH 4 and plotted against total dendrimer concentration (Figure 42). The simulated profile was hyperbolic wherein the fraction of bound drug increased with total drug concentration, and then plateaued. The plateau region indicated the optimum concentration of dendrimer needed to provide the yield of dendrimer-drug complex. Simulations predict that a 90% yield of bound drug

can be achieved using a total concentration of dendrimer ≥ 0.057 μM. The dendrimer concentration range used in this study produced a 28 % of yield of bound daptomycin bound. Whereas, the predicted fraction of bound drug as a function of total dendrimer concentration can be increased by changing the total daptomycin concentration from 2 to 5 μM. Taken together these simulations suggest that greater than 90% of the total drug concentration can be bound using dilute solutions of dendrimer and daptomycin. Whether these preparations can be scaled up to provide therapeutically-useful delivery system designs has yet to be determined.

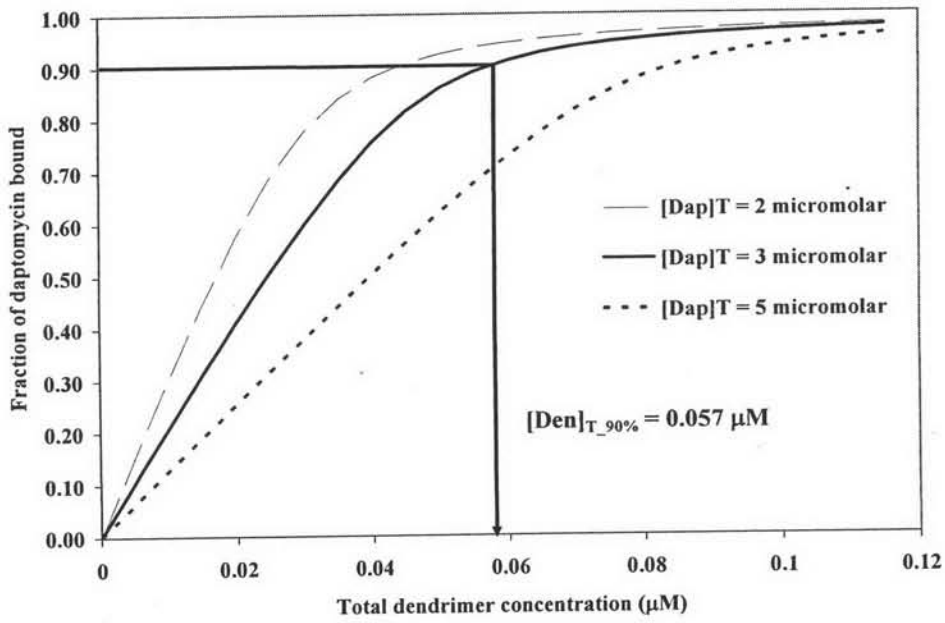

Figure 42 Predicted profiles of fraction of daptomycin bound as function of total dendrimer concentration using the condition of the titration between PAMAM generation 6 with daptomycin at pH 4.